vators of the ubiquitin-proteasome pathway, or a combination of the two have therapeutic potential for fALS. In conclusion, our results demonstrate that mutant SOD1 is degraded by at least two pathways, macroautophagy and the proteasome pathway, and that the clearance of mutant SOD1 by macroautophagy reduces its cell toxicity. These findings may provide insight into the molecular mechanisms of the pathogenesis of fALS.

Acknowledgments—We thank Dr. Ryosuke Takahashi (Kyoto University) and Dr. Makoto Urushitani (Laval University) for the gift of pcDNA3-hSOD1 (wild-type and mutant A4V, G85R, and G93A) plasmids, and Naoki Takagaki for the support in English.

REFERENCES

1. Bruijn, L. I., Miller, T. M., and Cleveland, D. W. (2004) *Annu. Rev. Neurosci.* **27,** 723–749
2. Cleveland, D. W., and Rothstein, J. D. (2001) *Nat. Rev. Neurosci.* **2,** 806–819
3. Rosen, D. R., Siddique, T., Patterson, D., Figlewicz, D. A., Sapp, P., Hentati, A., Donaldson, D., Goto, J., O'Regan, J. P., Deng, H. X., Rahmani, Z., Krizus, A., McKenna-Yasek, D., Cayabyab, A., Gaston, S. M., Berger, R., Tanzi, R. E., Halperin, J. J., Herzfeldt, B., Van den Bergh, R., Hung, W. Y., Bird, T., Deng, G., Mulder, D. W., Smyth, C., Laing, N. G., Soriano, E., Pericak-Vance, M. A., Haines, J., Rouleau, G. A., Gusella, J. S., Horvitz, H. R., and Brown, R. H., Jr. (1993) *Nature* **362,** 59–62
4. Gurney, M. E., Pu, H., Chiu, A. Y., Dal Canto, M. C., Polchow, C. Y., Alexander, D. D., Caliendo, J., Hentati, A., Kwon, Y. W., Deng, H. X., Chen, W., Zhai, P., Sufit, R. L., and Siddique, T. (1994) *Science* **264,** 1772–1775
5. Reaume, A. G., Elliott, J. L., Hoffman, E. K., Kowall, N. W., Ferrante, R. J., Siwek, D. F., Wilcox, H. M., Flood, D. G., Beal, M. F., Brown, R. H., Jr., Scott, R. W., and Snider, W. D. (1996) *Nat. Genet.* **13,** 43–47
6. Goldberg, A. L. (2003) *Nature* **426,** 895–899
7. Cuervo, A. M. (2004) *Trends Cell Biol.* **14,** 70–77
8. Hoffman, E. K., Wilcox, H. M., Scott, R. W., and Siman, R. (1996) *J. Neurol. Sci.* **139,** 15–20
9. Johnston, J. A., Dalton, M. J., Gurney, M. E., and Kopito, R. R. (2000) *Proc. Natl. Acad. Sci. U. S. A.* **97,** 12571–12576
10. Niwa, J., Ishigaki, S., Hishikawa, N., Yamamoto, M., Doyu, M., Murata, S., Tanaka, K., Taniguchi, N., and Sobue, G. (2002) *J. Biol. Chem.* **277,** 36793–36798
11. Miyazaki, K., Fujita, T., Ozaki, T., Kato, C., Kurose, Y., Sakamoto, M., Kato, S., Goto, T., Itoyama, Y., Aoki, M., and Nakagawara, A. (2004) *J. Biol. Chem.* **279,** 11327–11335
12. Shringarpure, R., Grune, T., Mehlhase, J., and Davies, K. J. (2003) *J. Biol. Chem.* **278,** 311–318
13. Asher, G., Tsvetkov, P., Kahana, C., and Shaul, Y. (2005) *Genes Dev.* **19,** 316–321
14. Di Noto, L., Whitson, L. J., Cao, X., Hart, P. J., and Levine, R. L. (2005) *J. Biol. Chem.* **280,** 39907–39913
15. Komatsu, M., Waguri, S., Chiba, T., Murata, S., Iwata, J., Tanida, I., Ueno, T., Koike, M., Uchiyama, Y., Kominami, E., and Tanaka, K. (2006) *Nature* **441,** 880–884
16. Hara, T., Nakamura, K., Matsui, M., Yamamoto, A., Nakahara, Y., Suzuki-Migishima, R., Yokoyama, M., Mishima, K., Saito, I., Okano, H., and Mizushima, N. (2006) *Nature* **441,** 885–889
17. Komatsu, M., Waguri, S., Ueno, T., Iwata, J., Murata, S., Tanida, I., Ezaki, J., Mizushima, N., Ohsumi, Y., Uchiyama, Y., Kominami, E., Tanaka, K., and Chiba, T. (2005) *J. Cell Biol.* **169,** 425–434
18. Ravikumar, B., Duden, R., and Rubinsztein, D. C. (2002) *Hum. Mol. Genet.* **11,** 1107–1117
19. Urushitani, M., Kurisu, J., Tsukita, K., and Takahashi, R. (2002) *J. Neurochem.* **83,** 1030–1042
20. Kabuta, T., Hakuno, F., Asano, T., and Takahashi, S. (2002) *J. Biol. Chem.* **277,** 6846–6851
21. Lee, D. H., and Goldberg, A. L. (1998) *Trends Cell Biol.* **8,** 397–403
22. Ostrowska, H., Wojcik, C., Wilk, S., Omura, S., Kozlowski, L., Stoklosa, T., Worowski, K., and Radziwon, P. (2000) *Int. J. Biochem. Cell Biol.* **32,** 747–757
23. Meng, L., Mohan, R., Kwok, B. H., Elofsson, M., Sin, N., and Crews, C. M. (1999) *Proc. Natl. Acad. Sci. U. S. A.* **96,** 10403–10408
24. Garcia-Echeverria, C. (2002) *Mini Rev. Med. Chem.* **2,** 247–259
25. Qin, Z. H., Wang, Y., Kegel, K. B., Kazantsev, A., Apostol, B. L., Thompson, L. M., Yoder, J., Aronin, N., and DiFiglia, M. (2003) *Hum. Mol. Genet.* **12,** 3231–3244
26. Cuervo, A. M., Stefanis, L., Fredenburg, R., Lansbury, P. T., and Sulzer, D. (2004) *Science* **305,** 1292–1295
27. Kabeya, Y., Mizushima, N., Ueno, T., Yamamoto, A., Kirisako, T., Noda, T., Kominami, E., Ohsumi, Y., and Yoshimori, T. (2000) *EMBO J.* **19,** 5720–5728
28. Webb, J. L., Ravikumar, B., Atkins, J., Skepper, J. N., and Rubinsztein, D. C. (2003) *J. Biol. Chem.* **278,** 25009–25013
29. Blommaart, E. F., Luiken, J. J., Blommaart, P. J., van Woerkom, G. M., and Meijer, A. J. (1995) *J. Biol. Chem.* **270,** 2320–2326
30. Gutierrez, M. G., Master, S. S., Singh, S. B., Taylor, G. A., Colombo, M. I., and Deretic, V. (2004) *Cell* **119,** 753–766
31. Liang, X. H., Jackson, S., Seaman, M., Brown, K., Kempkes, B., Hibshoosh, H., and Levine, B. (1999) *Nature* **402,** 672–676
32. Shimizu, S., Kanaseki, T., Mizushima, N., Mizuta, T., Arakawa-Kobayashi, S., Thompson, C. B., and Tsujimoto, Y. (2004) *Nat. Cell Biol.* **6,** 1221–1228
33. Aquilano, K., Rotilio, G., and Ciriolo, M. R. (2003) *J. Neurochem.* **85,** 1324–1335
34. Kato, S., Takikawa, M., Nakashima, K., Hirano, A., Cleveland, D. W., Kusaka, H., Shibata, N., Kato, M., Nakano, I., and Ohama, E. (2000) *Amyotroph. Lateral Scler. Other Motor Neuron Disord.* **1,** 163–184
35. Bruijn, L. I., Becher, M. W., Lee, M. K., Anderson, K. L., Jenkins, N. A., Copeland, N. G., Sisodia, S. S., Rothstein, J. D., Borchelt, D. R., Price, D. L., and Cleveland, D. W. (1997) *Neuron* **18,** 327–338
36. Matsumoto, G., Stojanovic, A., Holmberg, C. I., Kim, S., and Morimoto, R. I. (2005) *J. Cell Biol.* **171,** 75–85
37. Lee, J. P., Gerin, C., Bindokas, V. P., Miller, R., Ghadge, G., and Roos, R. P. (2002) *J. Neurochem.* **82,** 1229–1238
38. Rabouille, C., Strous, G. J., Crapo, J. D., Geuze, H. J., and Slot, J. W. (1993) *J. Cell Biol.* **120,** 897–908
39. Pramatarova, A., Laganiere, J., Roussel, J., Brisebois, K., and Rouleau, G. A. (2001) *J. Neurosci.* **21,** 3369–3374
40. Lino, M. M., Schneider, C., and Caroni, P. (2002) *J. Neurosci.* **22,** 4825–4832
41. Clement, A. M., Nguyen, M. D., Roberts, E. A., Garcia, M. L., Boillee, S., Rule, M., McMahon, A. P., Doucette, W., Siwek, D., Ferrante, R. J., Brown, R. H., Jr., Julien, J. P., Goldstein, L. S., and Cleveland, D. W. (2003) *Science* **302,** 113–117
42. Urushitani, M., Sik, A., Sakurai, T., Nukina, N., Takahashi, R., and Julien, J. P. (2006) *Nat. Neurosci.* **9,** 108–118
43. Arrasate, M., Mitra, S., Schweitzer, E. S., Segal, M. R., and Finkbeiner, S. (2004) *Nature* **431,** 805–810
44. Saudou, F., Finkbeiner, S., Devys, D., and Greenberg, M. E. (1998) *Cell* **95,** 55–66
45. Schaffar, G., Breuer, P., Boteva, R., Behrends, C., Tzvetkov, N., Strippel, N., Sakahira, H., Siegers, K., Hayer-Hartl, M., and Hartl, F. U. (2004) *Mol. Cell.* **15,** 95–105
46. Nucifora, F. C., Jr., Sasaki, M., Peters, M. F., Huang, H., Cooper, J. K., Yamada, M., Takahashi, H., Tsuji, S., Troncoso, J., Dawson, V. L., Dawson, T. M., and Ross, C. A. (2001) *Science* **291,** 2423–2428

The American Journal of Pathology, Vol. 169, No. 5, November 2006

DOI: 10.2352/ajpath.2006.060301

Metabolic, Endocrine and Genitourinary Pathobiology

Localization of Ubiquitin C-Terminal Hydrolase L1 in Mouse Ova and Its Function in the Plasma Membrane to Block Polyspermy

Satoshi Sekiguchi,* Jungkee Kwon,†‡ Etsuko Yoshida,§ Hiroko Hamasaki,* Shizuko Ichinose,¶ Makoto Hideshima,* Mutsuki Kuraoka,* Akio Takahashi,† Yoshiyuki Ishii,* Shigeru Kyuwa,* Keiji Wada,† and Yasuhiro Yoshikawa*

From the Department of Biomedical Science, Graduate School of Agricultural and Life Sciences, University of Tokyo, Tokyo, Japan; the Department of Degenerative Neurological Disease‡ and the Section of Laboratory Animal Resources,§ National Institute of Neuroscience, National Center of Neurology and Psychiatry, Tokyo, Japan; the Instrumental Analysis Research Center for Life Science,¶ Tokyo Medical and Dental University, Tokyo, Japan; and the Laboratory of Animal Medicine,‡ College of Veterinary Medicine, Chonbuk National University, Jeonju, Korea*

Protein degradation is essential for oogenesis and embryogenesis. The ubiquitin-proteasome system regulates many cellular processes via the rapid degradation of specific proteins. Ubiquitin carboxyl-terminal hydrolase L1 (UCH-L1) is exclusively expressed in neurons, testis, ovary, and placenta, each of which has unique biological activities. However, the functional role of UCH-L1 in mouse oocytes remains unknown. Here, we report the expression pattern of UCH-L1 and its isozyme UCH-L3 in mouse ovaries and embryos. Using immunocytochemistry, UCH-L1 was selectively detected on the plasma membrane, whereas UCH-L3 was mainly detected in the cytoplasm, suggesting that these isozymes have distinct functions in mouse eggs. To further investigate the functional role of UCH-L1 in mouse eggs, we analyzed the fertilization rate of UCH-L1-deficient ova of *gad* female mice. Female *gad* mice had a significantly increased rate of polyspermy in *in vitro* fertilization assays, although the rate of fertilization did not differ significantly from wild-type mice. In addition, the litter size of *gad* female mice was significantly reduced compared with wild-type mice. These results may identify UCH-L1 as a candidate for a sperm-oocyte interactive binding or fusion protein on the plasma membrane that functions during the block to polyspermy in mouse oocytes. ***(Am J Pathol 2006, 169:1722–1729; DOI: 10.2352/ajpath.2006.060301)***

Ubiquitin C-terminal hydrolase L1 (UCH-L1) is one of many deubiquitinating enzymes and is selectively and abundantly expressed in the ovary, placenta, testis, and neuronal cells.[1–6] Recent studies suggest that UCH-L1 associates with monoubiquitin and prolongs ubiquitin half-life in neurons.[7] Our previous work on UCH-L1 function in *gad* mice suggests that these mice are resistant to apoptotic stress in retinal cells and testicular germ cells.[8,9] This observation is consistent with a recent report that the overexpression of UCH-L1 induces testicular germ cell apoptosis in *Uchl1* transgenic mice.[10] Furthermore, both UCH-L1 and UCH-L3, the predominant functional UCHs, are differentially expressed in testis during spermatogenesis. These results demonstrate that these enzymes have distinct functions in the testis and epididymis after apoptotic stress,[9,11] even though they have high (52%) amino acid sequence identity.[12]

The above data are in accordance with a number of studies that have linked inhibition of the ubiquitin-proteasome system (UPS) with suppression of apoptosis.[8,13–15] UCH-L1 is an important enzyme for UPS-dependent proteolysis and plays a regulatory role in the cell cycle and cellular proliferation. Thus, its expression in placenta is of

Supported by the Japan Society (research fellowship to S.S.); grants-in-aid for scientific research from the Ministry of Health, Labour, and Welfare of Japan; grants-in-aid for scientific research from the Ministry of Education, Culture, Sports, Science, and Technology of Japan; the Program for Promotion of Fundamental Studies in Health Sciences of the National Institute of Biomedical Innovation; the Japan Science and Technology Agency; and in part by the Brain Korea 21 project 2006.

S.S. and J.K. are joint first authors.

K.W. and Y.Y. contributed equally to this study.

Accepted for publication August 3, 2006.

Address reprint requests to Yasuhiro Yoshikawa, Department of Biomedical Science, Graduate School of Agricultural and Life Sciences, University of Tokyo, 1-1-1 Yayoi, Bunkyo-ku, Tokyo 113-8657, Japan. E-mail: ayyoshi@mail.ecc.u-tokyo.ac.jp.

considerable interest.[3,4] Recent studies reported that UPS controls the degradation of various substrates during gametogenesis and fertilization,[16–19] but relatively little is known about the functional role of the UPS in fertilization. UCH-L1 is expressed in oocytes in ovaries.[5,20] Oocytes, as well as spermatogonia in testis, have multiple potentials and activities for development. However, the function of UCH-L1 during oogenesis is unclear. RFPL4 (ret finger protein-like 4) and FAM (fat facets in mouse) are involved in regulating oogenesis.[21,22] RFPL4 is highly expressed during oogenesis and functions as an E3 ubiquitin ligase to target proteins for proteasomal degradation.[21] FAM is a developmentally regulated substrate-specific deubiquitinating enzyme that is required for preimplantation of the mouse embryo.[22] Thus, the UPS might be important during oocyte development and differentiation of the embryo after fertilization.

Here, we analyzed the functional role of UCH-L1 using mouse oocytes and embryos. Our results indicate that UCH-L1 is selectively expressed on the plasma membrane of mouse ova, where it may regulate membrane penetration by spermatozoa. In addition, the unique expression patterns of UCH-L1 and UCH-L3 suggest that these proteins have distinct functions during oogenesis and embryogenesis. Our results therefore provide strong evidence that UCH-L1 functions in the polyspermy block during mammalian fertilization.

Materials and Methods

Animals

We used 8-week-old BDF1, *gad* (CBA/RFM),[23,24] and *Uchl3* knockout (C57BL/6J)[12,25] female and male mice. BDF1 mice were purchased from Nihon SLC, Inc. (Hamamatsu, Japan). The *gad* mouse is an autosomal recessive mutant that was obtained by crossing CBA and RFM mice. The *gad* line was maintained by intercrossing for more than 20 generations.[23,24] The *Uchl3* knockout mouse was generated by standard methods using homologously recombinant ES cells from 129SV mice.[12,25] The knockout line was back-crossed several times with C57BL/6J mice. *gad* mice were maintained at our institute, and *Uchl3* knockout mice were maintained at the National Institute of Neuroscience, National Center of Neurology and Psychiatry (Tokyo, Japan). Animal care and handling were in accordance with institutional regulations and were approved by the Animal Care and Use Committee of the University of Tokyo.

Oocyte Collection and in Vitro Fertilization

Female mice were superovulated by intraperitoneal injections with 5 IU of pregnant mare serum gonadotropin (Sankyo, Tokyo, Japan) for 48 hours, followed by 5 IU of human chorionic gonadotropin (Sankyo). Ovulated eggs were collected from the ampullae of oviducts by the scratching method 16 hours after human chorionic gonadotropin injection and placed in 400-μl droplets of Toyoda, Yokoyama, and Hoshi (TYH)[26] containing 0.4 mg/ml bovine serum albumin (Sigma-Aldrich, St. Louis, MO). Spermatozoa were collected from the cauda epididymis of male mice and preincubated for 1 hour in 400 μl of TYH to allow capacitation before insemination. After capacitation, the sperms were introduced into the fertilization medium at a final concentration of 150 spermatozoa/μl. At 4 hours after insemination, 0.05% hyaluronidase (Sigma-Aldrich) was added to the medium for 5 minutes. The eggs were washed thoroughly three times and then cultured in potassium simplex optimized medium (KSOM).[26] After fertilization, all embryos were incubated in a humidified atmosphere of 5% CO_2 in air at 37°C in 100-μl drops of KSOM overlaid with mineral oil. To analyze fertilization in *gad* mice, *gad* (n = 5) and wild-type (CBA/RFM) (n = 5) female mice were superovulated. Ovulated oocytes of *gad* and wild-type mice were fertilized with wild-type spermatozoa.

Western Blotting

Total protein of ovary extracts (10 μg/lane), oocytes, or embryos (20 oocytes or embryos per lane) was subjected to sodium dodecyl sulfate-polyacrylamide gel electrophoresis using 12.5% gels. Proteins were electrophoretically transferred to polyvinylidene difluoride membranes (Bio-Rad, Hercules, CA) and blocked with 1% bovine serum albumin in TBS-T [50 mmol/L Tris base, pH 7.5, 150 mmol/L NaCl, and 0.1% (w/v) Tween 20]. The membranes were incubated individually with primary antibodies against UCH-L1, UCH-L3,[2] monoubiquitin (U5379, Sigma-Aldrich), zona pellucida 2 (ZP2; Santa Cruz Biotechnology, Santa Cruz, CA), and zona pellucida 3 (ZP3) (Santa Cruz Biotechnology). After thorough rinsing, blots were further incubated with peroxidase-conjugated goat anti-rabbit IgG (DakoCytomation, Glostrup, Denmark) for 1 hour at room temperature. Immunoreactions were visualized by enhanced chemiluminescence (ECL Plus; GE Healthcare UK Ltd. Amersham Place, Little Chalfont, Buckinghamshire, UK). Each immunoreactive band was quantified using commercially available software (Quantity One; PDI, Upper Saddle River, NJ). Negative control extracts of ovary or oocytes were obtained from *gad* and *Uchl3* knockout mice.

Histological and Immunochemical Assessment

Ovaries of BDF1 female and *gad* mice were fixed in 4% paraformaldehyde, embedded in paraffin wax, and then sectioned at 4-μm thickness. Ovary sections of *gad* mice were stained with hematoxylin and eosin (H&E). Light microscopy was used for routine observations. For immunohistochemical staining, the sections were incubated with Block Ace (Dainippon Sumitomo Pharma, Osaka, Japan) for 1 hour at room temperature followed by incubation overnight at 4°C with a rabbit polyclonal antibody against UCH-L1 and UCH-L3.[2] The sections were then incubated with biotinylated goat anti-rabbit IgG (DAKO), which was followed by incubation with streptavidin-biotin-horseradish peroxidase complex (sABC kit; DAKO). Immunoreactivity was visualized by treating the sections

with 3,3′-diaminobenzidine tetroxide (Dojin Kagaku, Kumamoto, Japan). Finally, the sections were counterstained with hematoxylin. Negative control ovaries were obtained from *gad* and *Uchl3* knockout mice.

For immunocytochemical staining, whole oocytes or embryos were fixed for 30 minutes with 4% paraformaldehyde in phosphate-buffered saline (PBS) and 0.2% (w/v) Triton X-100 (ICN Biomedicals, Aurora, OH) in PBS for 30 minutes. Nonspecific binding of immunoglobulins was blocked by incubation with Block Ace (Dainippon Pharmaceutical, Ltd.) for 1 hour at room temperature. The sections were then incubated with primary antibodies against UCH-L1, UCH-L3, and lectin with Rhodamine-Lens Culinaris Agglutinin (Vector Laboratories, Burlingame, CA). The sections were then incubated with Alexa 488-conjugated goat anti-rabbit IgG (Molecular Probes, Eugene, OR) and propidium iodide (Molecular Probes). Stained sections were observed under a confocal laser microscope (Laser Scanning Microscope 510; Carl Zeiss, Jena, Germany). Negative control oocytes were obtained from *gad* and *Uchl3* knockout mice by superovulation.

Quantitative Analysis

Normal oocytes were identified by the presence of the first polar body.[27,28] The frequency of normal oocytes was calculated by counting the normal oocytes in the total superovulated oocytes of *gad* (n = 173) and wild-type (n = 148) mice. To determine the fertilization rate, putative fertilized eggs (by *in vitro* fertilization) were fixed in acetic alcohol (1:3, glacial acetic acid/ethanol) and then stained with 1% aceto-orcein to visualize pronuclei and assess sperm penetration and incidence of monospermic and polyspermic fertilization. Polyspermic fertilization was defined as the presence of three or more pronuclei. The rate of polyspermic fertilization was calculated by counting the polyspermic eggs among the total fertilized eggs of *gad* (n = 71) and wild-type (n = 56) mice.

Electron Microscopic Analysis

Ovulated mature oocytes and zygotes of BDF1 mice were fixed with 4% paraformaldehyde, and frozen sections were prepared for electron microscopy. The sections were incubated with an antibody against UCH-L1.[2] Subsequently, the ABC method was performed as indicated by the supplier, and the peroxidase reaction was developed in diaminobenzidine. Immunostained sections were fixed in 2.5% glutaraldehyde, postfixed in 1% OsO_4, dehydrated in a graded series of ethanol, and embedded in Epon 812.[29] Ultrathin sections were cut with an ultramicrotome, stained with uranyl acetate,[29] and examined with an electron microscope H-7100 (Hitachi, Hitachinaka, Japan).

Breeding Test of gad Female Mice

gad (n = 12) and wild-type (CBA/RFM) (n = 15) female mice and wild-type (CBA/RFM) (n = 9) male mice were subjected to a breeding study. Three female mice of the same genotype were housed with one male mouse per cage. Cages were monitored daily at midday, and the appearance of a vaginal plug was recognized as day 0.5 of gestation. The number of pups, litters, and litter size of *gad* and wild-type female mice were recorded.

Statistical Analysis

The mean and SD were calculated for all data (presented as mean ± SD). The Student's t-test was used for all statistical analyses.

Results

Expression of UCH-L1 and UCH-L3 in Mouse Ovaries

We first used Western blotting to address whether both UCH-L1 and UCH-L3 levels are expressed in ovaries during proestrus, estrus, metestrus, and diestrus (Figure 1A). Both proteins were detected at all estrous cycle stages in wild-type mice. As expected, UCH-L1 was not detected in *gad* ovaries and UCH-L3 was not detected in *Uchl3* knockout ovaries. The levels of UCH-L1 and UCH-L3 in ovaries did not change throughout the estrous cycle (Figure 1A).

We next used immunohistochemistry to address whether both UCH-L1 and UCH-L3 are present in developing follicles (primordial, primary, secondary, tertiary, and mature follicles; Figure 1B). In the ovary, UCH-L1 staining was most intense at the plasma membrane of oocytes in developing follicles (Figure 1B, a–e), whereas UCH-L3 staining was concentrated in the cytoplasm of oocytes (Figure 1B, g–k). The oocytes of *gad* and *Uchl3* knockout mice ovaries were negative for UCH-L1 and UCH-L3, respectively (Figure 1B, f and l).

Expression of UCH-L1 and UCH-L3 in Mouse Mature Oocytes and Preimplantation Embryos

Using Western blotting, we examined the levels of both UCH-L1 and UCH-L3 in mature oocytes and during embryogenesis (zygote, two cells, four cells, eight cells, morulas, and blastocysts). UCH-L1 and UCH-L3 were detected in mature oocytes and during all of the embryonic stages we tested; the level of UCH-L1 was essentially constant in all cases, but the level of UCH-L3 was lower in the blastocyst stage (Figure 2A).

We further analyzed the distribution of UCH-L1 and UCH-L3 in ovulated mature oocytes and during embryogenesis using immunocytochemistry (Figure 2B). UCH-L1 immunoreactivity was intense on the plasma membrane of oocytes and developing embryos but not in the cytoplasm of eggs (Figure 2B, a–g). Furthermore, UCH-L1 immunoreactivity was observed continuously during embryogenesis (Figure 2B, c–g). In the blastocyst stage, UCH-L1 was observed in the outer layer cells of the trophectoderm (Figure 2B, g). UCH-L3 immunoreac-

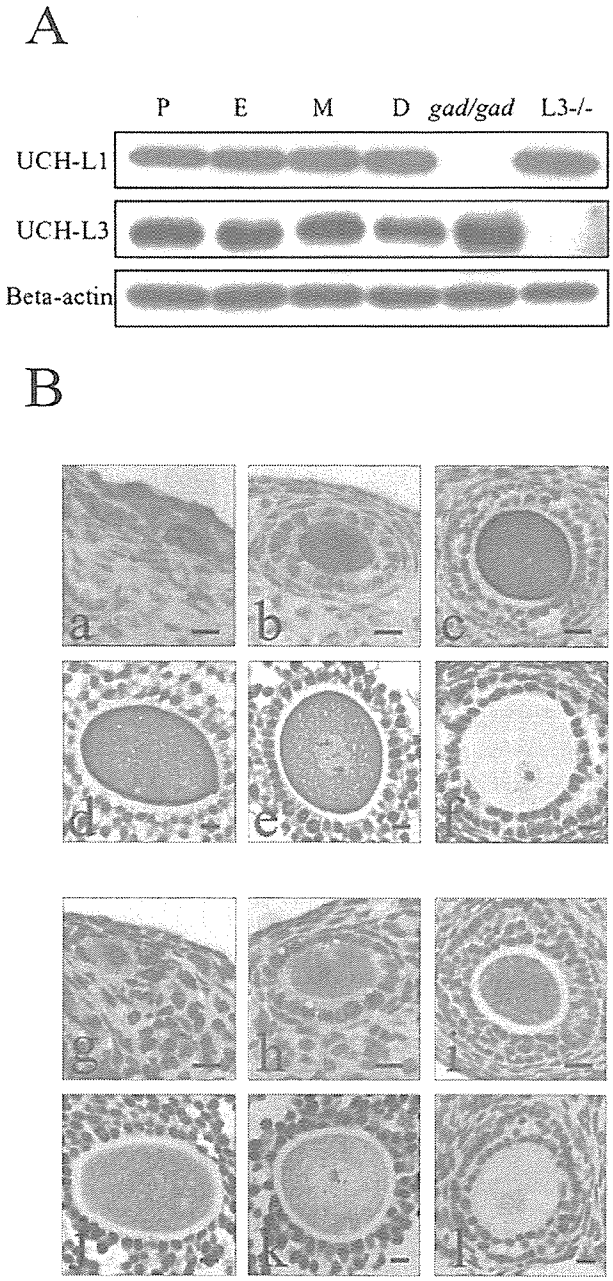

Figure 1. Expression of UCH-L1 and UCH-L3 in mouse ovaries. **A:** Western blotting analysis of UCH-L1 and UCH-L3 in ovaries during the estrous cycle. Proestrus (P), estrus (E), metestrus (M), and diestrus (D) ovaries; *gad/gad* and $L3^{-/-}$ represent *gad* and *Uchl3* knockout mouse ovaries, respectively. **B:** Immunohistochemical analyses of UCH-L1 (**a–e**) and UCH-L3 (**g–k**) in BDF1 mouse ovaries (**a–e**, **g–k**). Ovaries from *gad* (**f**) and *Uchl3* knockout mice (**l**) are negative controls. UCH-L1 is highly expressed on the plasma membrane of oocytes. UCH-L3 is diffusely expressed in the cytoplasm of oocytes. Follicle stages: primordial (**a**, **g**), primary (**b**, **h**), secondary (**c**, **i**), tertiary (**d**, **j**), and mature (**e**, **k**) from BDF1 mouse ovaries. Scale bars = 10 μm.

tivity was seen in the cytoplasm of oocytes and developing embryos (Figure 2B, i–o), as was detected in ovaries (Figure 2A). In the blastocyst stage, UCH-L3 was observed in the inner cells (Figure 2B, o). The oocytes and developing embryos of *gad* and *Uchl3* knockout mice were negative for UCH-L1 and UCH-L3, respectively (Figure 2B, h and p).

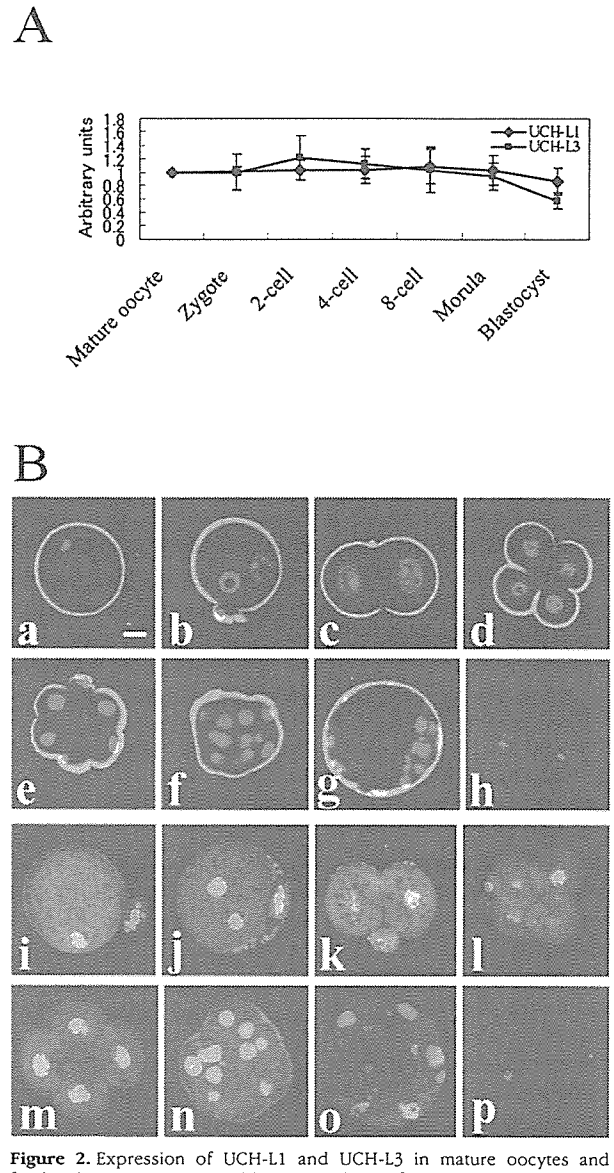

Figure 2. Expression of UCH-L1 and UCH-L3 in mature oocytes and fertilized eggs. **A:** Western blotting analysis of UCH-L1 and UCH-L3 in ovulated mature oocytes and developing eggs of BDF1 mice. **B:** Immunocytochemical analysis of UCH-L1 (**a–g**) and UCH-L3 (**i–o**) in ovulated mature oocytes and developing embryos of BDF1 mice (**a–g**, **i–o**). Ovulated mature oocytes of *gad* (**h**) and *Uchl3* knockout mice (**p**) are negative controls. UCH-L1 immunoreactivity was seen only on the plasma membrane of mature oocytes (**a**) and developing eggs (**b–g**). UCH-L3 immunoreactivity was seen in the cytoplasm of oocytes (**j**) and developing eggs (**j–o**). Stages: oocytes (**a**, **i**), zygotes (**b**, **j**), two cells (**c**, **k**), four cells (**d**, **l**), eight cells (**e**, **m**), morulas (**f**, **n**), and blastocyst (**g**, **o**). Nuclei are shown in red. Scale bar = 20 μm.

Immunoelectron Microscopy

The cortical granule is located right under the plasma membrane in oocytes. This organelle is unique to oocytes and plays an important role in fertilization. At the light microscope level, it is difficult to determine whether UCH-L1 immunoreactivity localizes to the plasma membrane or cortical granule. To address this issue, we investigated the subcellular localization of UCH-L1 in ovulated mature oocytes and zygotes at the ultrastructural level (Figure 3). Intense UCH-L1 immunoreactivity was

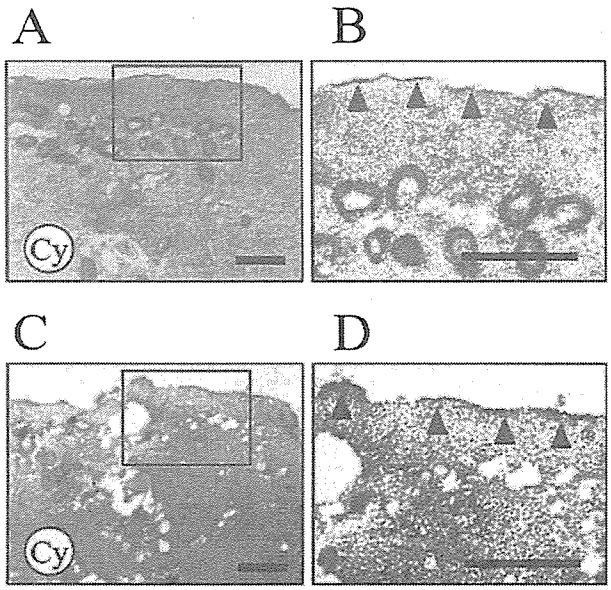

Figure 3. Localization of UCH-L1 on the plasma membrane in mature oocytes and zygotes by immunoelectron microscopy. **A–D:** Mature oocyte and zygote of BDF1 mouse are immunostained with UCH-L1. **B** and **D:** Magnified images of the region enclosed by small rectangles in **A** and **C**. UCH-L1 immunoreactivity is intense on the plasma membrane (**arrowheads**) of an ovulated mature oocyte (**B**) and zygote (**D**). The position of cytoplasm (Cy) is indicated. Scale bars = 1 μm.

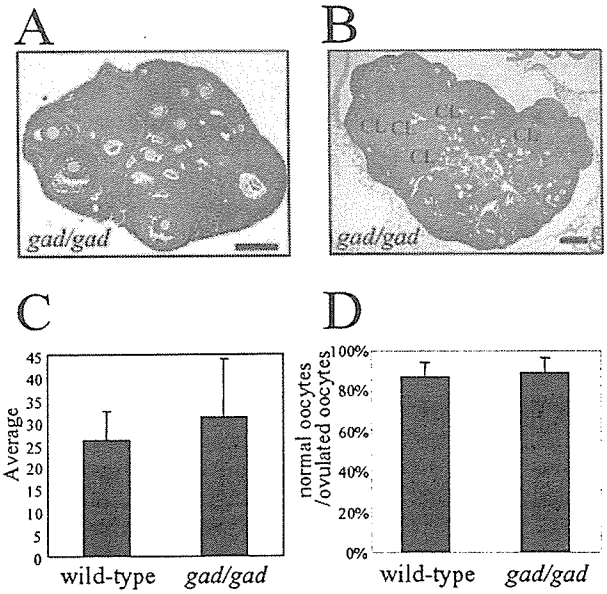

Figure 4. Histology of ovaries and the ovulation rate of *gad* mice. **A** and **B:** Ovarian sections of *gad* mice stained with H&E. *gad* mouse ovaries have morphologically normal oocytes, follicles, and corpora lutea (CL). **C** and **D:** The average number of superovulated oocytes (**C**) and the normal oocyte rate (normal oocytes/total ovulated oocytes) (**D**) in *gad* mice are not significantly different from wild-type mice. Scale bars = 200 μm.

observed on the plasma membrane of ovulated mature oocytes (Figure 3, A and B) and zygotes (Figure 3, C and D). However, the intensity of the plasma membrane immunoreactivity was greater in mature oocytes than in zygotes. Therefore, we concluded that the distribution of UCH-L1 may change after fertilization.

Morphology of the gad Ovaries and Ovulated Oocytes

To assess whether *gad* mice have morphologically normal ovaries, we used histology to compare ovaries from *gad* and wild-type (CBA/RFM) mice. *gad* mouse ovaries had morphologically normal oocytes, follicles, and corpora lutea (Figure 4, A and B). In addition, *gad* mice had a normal estrous cycle (data not shown). We further assessed *gad* mouse ovarian function by comparison with wild-type mice using the ovulation test. The total number of ovulated oocytes and the normal oocyte ovulation rate of superovulated oocytes did not differ significantly between *gad* mice and wild-type mice (Figure 4, C and D).

High Polyspermy Rate in gad Mouse Oocytes

To analyze the fertilization rate in UCH-L1-deficient embryos of *gad* female mice, we assessed fertilization by *in vitro* fertilization using wild-type spermatozoa. For mice, the presence of more than three or more pronuclei defines polyspermic fertilization. Fertilized eggs from *gad* mice had characteristics consistent with this definition of polyspermy (Figure 5, B and C). By contrast, wild-type eggs showed normal zygotic nuclei (Figure 5A). The fertilized eggs of *gad* mice had a significantly higher rate of polyspermy (27 ± 0.04%) compared with wild-type mice (2 ± 0.02%) (Figure 5E). However, the fertility of *gad* mouse eggs (46 ± 0.06%) did not differ significantly from that of wild-type mice (43 ± 0.09%) (Figure 5D).

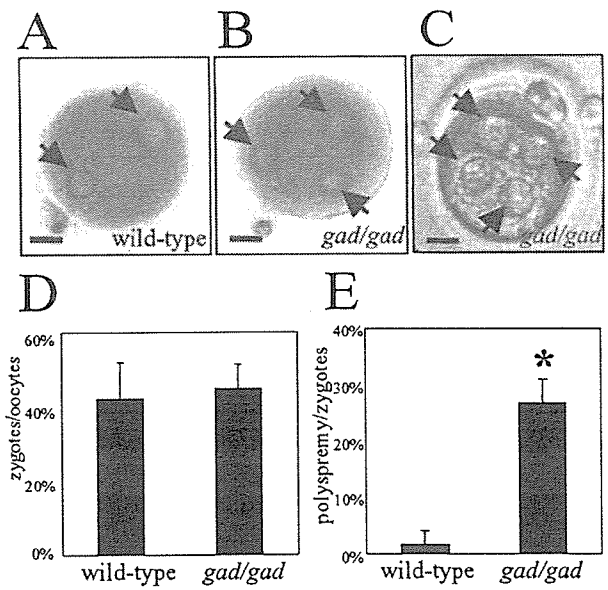

Figure 5. Incidence of polyspermy in *gad* mice. Fertilized eggs were stained with aceto-orcein (**A, B**) or visualized by inverted microscopy (**C**). **A:** Normal fertilized egg with two pronuclei (**arrows** in **A–C**) in wild-type mice. **B** and **C:** Polyspermic fertilized eggs in *gad* mice have three or four pronuclei. **D:** The fertility rate in *gad* mice is not significantly different from wild-type mice. **E:** Polyspermic rate in *gad* mice is significantly higher than that of wild-type mice. $^{*}P < 0.01$. Scale bars = 20 μm.

Table 1. Breeding Study of *gad* and Wild-Type Female Mice with Wild-Type Male Mice

Genotype (*n*)	Litters	Pups	Litter size
Wild type (15)	15	99	6.6 ± 1.3
gad/gad (12)	11	33	3 ± 2.0*

Results represent the mean ± SD.
*Significantly different from wild-type mice, $P < 0.001$.

Low Breeding Rate of gad Female Mice

To further evaluate the high polyspermic fertilization rate of *gad* female mice, we characterized the litter size of these mice after mating with wild-type male mice. *gad* female mice exhibited normal puberty and estrous cycle, as assessed by vaginal opening and vaginal smear, but they had reduced fertility, as evidenced by a significant decrease in litter size (3 ± 2.0) compared with wild-type mice (6.6 ± 1.3) (Table 1).

Monoubiquitin Level in gad Mouse Oocytes

Our previous study demonstrated that UCH-L1 stabilizes monoubiquitin in testes and that the level of monoubiquitin is decreased in male *gad* mice.[8,9] To determine whether the high polyspermy rate in *gad* mouse oocytes correlated with a reduced level of monoubiquitin in the oocytes, we used Western blotting to measure monoubiquitin levels in oocytes from *gad* mice and wild-type mice. The monoubiquitin level was substantially lower in *gad* mouse oocytes (Figure 6A). However, wild-type and *gad* mouse oocytes showed the normal zona reaction (postfertilization proteolytic cleavage of ZP2) and normal cortical reaction (postfertilization exocytosis of cortical granules) (Figure 6, B and C).

Discussion

Polyspermy refers to the penetration of more than one sperm into oocytes during fertilization and is currently considered a pathological phenomenon in mammals.[30] However, an exceptionally high incidence of polyspermic fertilization has been revealed in pig fertilization.[31,32] The reasons for this higher incidence of polyspermy in oocytes are not clear, and relatively little is known about the exact mechanisms that prevent polyspermy. The mechanism that prevents polyspermy is classically illustrated by the zona reaction (cortical reaction) and subsequent plasma membrane block.[33,34] After penetration by sperm, the zona reaction occurs, and cortical contents are extruded into the perivitelline space, thereby preventing polyspermic penetration by hardening of the zona pellucida.[35] Plasma membrane block is assumed to result from changes (eg, the destruction of sperm receptors in the membrane) that preclude sperm adherence.[36,37]

Recent studies have demonstrated that the UPS is responsible for extracellular degradation of the sperm receptor on the outer face of zona pellucida and that proteasomal inhibitors block sperm penetration of the zona pellucida during fertilization.[17–19] These findings

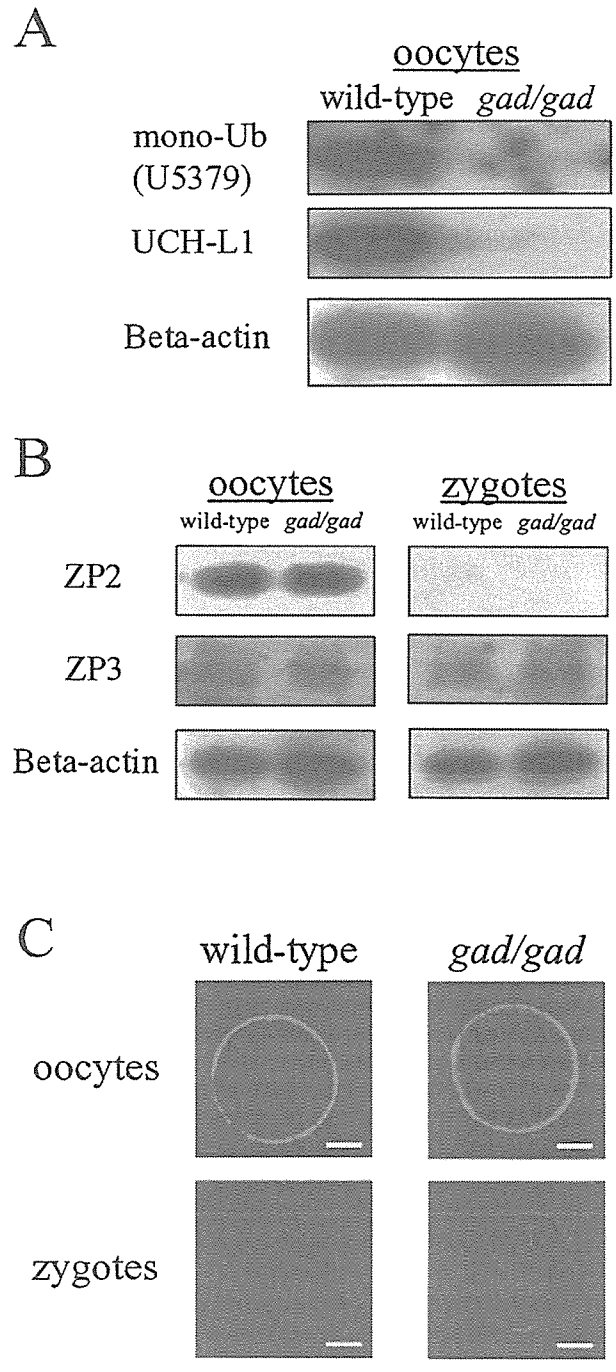

Figure 6. Expression of monoubiquitin, zona reaction, and cortical reaction in *gad* mice. **A:** Western blotting analysis of monoubiquitin of wild-type and *gad* mouse oocytes. The monoubiquitin protein level is substantially lower in *gad* than in wild-type. **B:** Western blotting analysis of ZP2 and ZP3 of wild-type and *gad* mouse oocytes and zygotes. Disappearance of ZP2 of zygotes because of postfertilization proteolytic cleavage is observed in wild-type and *gad* mice. **C:** Cortical reaction analysis of wild-type and *gad* mouse oocytes and zygotes. Disappearance of rhodamine-LCA of zygotes because of postfertilization cortical granule exocytosis is observed in wild-type and *gad* mice. Scale bars = 20 μm.

strongly support a role for the UPS in the sperm-oocyte interaction of the zona pellucida. However, our results showed the apparent contradiction that the high incidence of polyspermy was caused by down-regulation of the UPS function distinct from previous studies.[17–19] Our

present work shows that UCH-L1 is exclusively localized on the oocyte plasma membrane and that UCH-L1-deficient embryos of *gad* female mice have a significantly increased polyspermy rate *in vitro* (Figures 2B and 5). These results suggest that UCH-L1 may modify plasma membrane components, thereby preventing multiple sperm entry. In mammals, it has been suggested that UCH-L1 associates with monoubiquitin[7,10]; moreover, the monoubiquitin pool is reduced in *gad* mice relative to wild-type mice. We have shown that the monoubiquitin level in *gad* mouse oocytes is substantially reduced relative to that of wild-type mice (Figure 6A). These results suggest that the high incidence of polyspermy in *gad* mice may have its basis in the down-regulation of the UPS because of a reduction in available monoubiquitin at the plasma membrane, even though *gad* mouse oocytes undergo a normal zona reaction (Figure 6, B and C).[30,38] In addition, *gad* mice also have morphologically normal ovary development and a normal rate of ovulation compared with wild-type mice (Figure 4).

CD9 is an integral membrane protein associated with integrins and other membrane proteins.[39] CD9 is extensively localized on the oocyte plasma membrane.[39–41] Recent studies suggest that CD9 participates in sperm-oocyte fusion in the mouse.[39] CD9 knockout female mice ovulate normally, but the oocytes are rarely fertilized because CD9 deficiency on the plasma membrane inhibits sperm-oocyte fusion. Many plasma membrane channels, transporters, and receptors undergo ubiquitination at the extracellular face, which is required for internalization and subsequent entry into the endocytic pathway.[42] These studies indicate that ubiquitination (monoubiquitination, multiple monoubiquitination, or polyubiquitination) of plasma membrane proteins might facilitate plasma membrane block.

In the present study, we showed that both UCH-L1 and UCH-L3 are strongly expressed throughout all stages of oogenesis and embryogenesis (Figure 1A), even though ovarian and uterine functions change periodically because of fluctuations in hormone levels.[43–45] Our previous studies suggested that UCH-L1 and UCH-L3, despite their high sequence homology,[12] have distinct expression patterns and differential function in testis and epididymis.[9,11] Here we show that these two proteins have distinct distributions: UCH-L1 is exclusively expressed on the plasma membrane of oocytes and embryos, whereas UCH-L3 is diffusely expressed in the cytoplasm (Figures 1B and 2B). Therefore, it is conceivable that UCH-L1 and UCH-L3 have different functional roles in oocytes and embryos, as was shown in the testis/epididymis.[9,11] Although our studies show that UCH-L3 is highly expressed in the cytoplasm of oocytes and embryos, we found no difference in the fertilization rate and litter size in *Uchl3* knockout female mice compared with wild-type (C57BL/6J) female mice (data not shown). Thus, UCH-L3 may not impact these developmentally related processes; further research is necessary to elucidate the cytoplasmic function of this UCH.

Polyspermy in humans mostly results in embryonic lethality or triploid embryos, which usually mature into infertile offspring.[46,47] According to the World Health Organization, ~80 million people worldwide are infertile. Infertility may result from female- or male-derived factors, a combination of the two, or as yet unidentified biological factors.[48] Our present work shows that a deficiency in UCH-L1 may be a new cause of female infertility. Thus, *gad* mice may be a useful model for further studies of infertility.

In conclusion, we show that UCH-L1-deficient *gad* female mice oocytes have a significantly increased rate of polyspermy in an *in vitro* fertilization assay; consequently, these mice have significantly decreased litter size. These results suggest that UCH-L1 is a crucial factor in the plasma membrane block to polyspermy in mouse oocytes.

Acknowledgments

We thank Kunihiko Naito and Koji Kashima (University of Tokyo) for technical assistance with *in vitro* fertilization.

References

1. Kwon J, Kikuchi T, Setsuie R, Ishii Y, Kyuwa S, Yoshikawa Y: Characterization of the testis in congenitally ubiquitin carboxy-terminal hydrolase-1 (Uch-L1) defective (gad) mice. Exp Anim 2003, 52:1–9
2. Kwon J, Wang YL, Setsuie R, Sekiguchi S, Sakurai M, Sato Y, Lee WW, Ishii Y, Kyuwa S, Noda M, Wada K, Yoshikawa Y: Developmental regulation of ubiquitin C-terminal hydrolase isozyme expression during spermatogenesis in mice. Biol Reprod 2004, 71:515–521
3. Sekiguchi S, Takatori A, Negishi T, Kwon J, Kokubo T, Ishii Y, Kyuwa S, Yoshikawa Y: Localization of ubiquitin carboxyl-terminal hydrolase-L1 in cynomolgus monkey placentas. Placenta 2005, 26:99–103
4. Sekiguchi S, Yoshikawa Y, Tanaka S, Kwon J, Ishii Y, Kyuwa S, Wada K, Nakamura S, Takahashi K: Immunohistochemical analysis of protein gene product 9.5, a ubiquitin carboxyl-terminal hydrolase, during placental and embryonic development in the mouse. Exp Anim 2003, 52:365–369
5. Wilson PO, Barber PC, Hamid QA, Power BF, Dhillon AP, Rode J, Day IN, Thompson RJ, Polak JM: The immunolocalization of protein gene product 9.5 using rabbit polyclonal and mouse monoclonal antibodies. Br J Exp Pathol 1988, 69:91–104
6. Kwon J, Mochida K, Wang YL, Sekiguchi S, Sankai T, Aoki S, Ogura A, Yoshikawa Y, Wada K: Ubiquitin C-terminal hydrolase L-1 is essential for the early apoptotic wave of germinal cells and for sperm quality control during spermatogenesis. Biol Reprod 2005, 73:29–35
7. Osaka H, Wang YL, Takada K, Takizawa S, Setsuie R, Li H, Sato Y, Nishikawa K, Sun YJ, Sakurai M, Harada T, Hara Y, Kimura I, Chiba S, Namikawa K, Kiyama H, Noda M, Aoki S, Wada K: Ubiquitin carboxy-terminal hydrolase L1 binds to and stabilizes monoubiquitin in neuron. Hum Mol Genet 2003, 12:1945–1958
8. Harada T, Harada C, Wang YL, Osaka H, Amanai K, Tanaka K, Takizawa S, Setsuie R, Sakurai M, Sato Y, Noda M, Wada K: Role of ubiquitin carboxy terminal hydrolase-L1 in neural cell apoptosis induced by ischemic retinal injury in vivo. Am J Pathol 2004, 164:59–64
9. Kwon J, Wang YL, Setsuie R, Sekiguchi S, Sato Y, Sakurai M, Noda M, Aoki S, Yoshikawa Y, Wada K: Two closely related ubiquitin C-terminal hydrolase isozymes function as reciprocal modulators of germ cell apoptosis in cryptorchid testis. Am J Pathol 2004, 165:1367–1374
10. Wang YL, Liu W, Sun YJ, Kwon J, Setsuie R, Osaka H, Noda M, Aoki S, Yoshikawa Y, Wada K: Overexpression of ubiquitin carboxyl-terminal hydrolase L1 arrests spermatogenesis in transgenic mice. Mol Reprod Dev 2006, 73:40–49
11. Kwon J, Sekiguchi S, Wang YL, Setsuie R, Yoshikawa Y, Wada K: The region-specific functions of two ubiquitin C-terminal hydrolase isozymes along the epididymis. Exp Anim 2006, 55:35–43
12. Kurihara LJ, Semenova E, Levorse JM, Tilghman SM: Expression and

functional analysis of Uch-L3 during mouse development. Mol Cell Biol 2000, 20:2498–2504
13. Rasoulpour RJ, Schoenfeld HA, Gray DA, Boekelheide K: Expression of a K48R mutant ubiquitin protects mouse testis from cryptorchid injury and aging. Am J Pathol 2003, 163:2595–2603
14. Yang Y, Yu X: Regulation of apoptosis: the ubiquitous way. FASEB J 2003, 17:790–799
15. Baarends WM, Wassenaar E, Hoogerbrugge JW, van Cappellen G, Roest HP, Vreeburg J, Ooms M, Hoeijmakers JH, Grootegoed JA: Loss of HR6B ubiquitin-conjugating activity results in damaged synaptonemal complex structure and increased crossing-over frequency during the male meiotic prophase. Mol Cell Biol 2003, 23:1151–1162
16. Baarends WM, Roest HP, Grootegoed JA: The ubiquitin system in gametogenesis. Mol Cell Endocrinol 1999, 151:5–16
17. Sutovsky P: Ubiquitin-dependent proteolysis in mammalian spermatogenesis, fertilization, and sperm quality control: killing three birds with one stone. Microsc Res Tech 2003, 61:88–102
18. Sutovsky P, Manandhar G, McCauley TC, Caamano JN, Sutovsky M, Thompson WE, Day BN: Proteasomal interference prevents zona pellucida penetration and fertilization in mammals. Biol Reprod 2004, 71:1625–1637
19. Sutovsky P, McCauley TC, Sutovsky M, Day BN: Early degradation of paternal mitochondria in domestic pig (Sus scrofa) is prevented by selective proteasomal inhibitors lactacystin and MG132. Biol Reprod 2003, 68:1793–1800
20. Ellederova Z, Halada P, Man P, Kubelka M, Motlik J, Kovarova H: Protein patterns of pig oocytes during in vitro maturation. Biol Reprod 2004, 71:1533–1539
21. Suzumori N, Burns KH, Yan W, Matzuk MM: RFPL4 interacts with oocyte proteins of the ubiquitin-proteasome degradation pathway. Proc Natl Acad Sci USA 2003, 100:550–555
22. Pantaleon M, Kanai-Azuma M, Mattick JS, Kaibuchi K, Kaye PL, Wood SA: FAM deubiquitylating enzyme is essential for preimplantation mouse embryo development. Mech Dev 2001, 109:151–160
23. Kikuchi T, Mukoyama M, Yamazaki K, Moriya H: Axonal degeneration of ascending sensory neurons in gracile axonal dystrophy mutant mouse. Acta Neuropathol (Berl) 1990, 80:145–151
24. Saigoh K, Wang YL, Suh JG, Yamanishi T, Sakai Y, Kiyosawa H, Harada T, Ichihara N, Wakana S, Kikuchi T, Wada K: Intragenic deletion in the gene encoding ubiquitin carboxy-terminal hydrolase in gad mice. Nat Genet 1999, 23:47–51
25. Kurihara LJ, Kikuchi T, Wada K, Tilghman SM, Semenova E, Levorse JM: Loss of Uch-L1 and Uch-L3 leads to neurodegeneration, posterior paralysis and dysphagia. Hum Mol Genet 2001, 10:1963–1970
26. Kito S, Hayao T, Noguchi-Kawasaki Y, Ohta Y, Hideki U, Tateno S: Improved in vitro fertilization and development by use of modified human tubal fluid and applicability of pronucleate embryos for cryopreservation by rapid freezing in inbred mice. Comp Med 2004, 54:564–570
27. Wang WH, Abeydeera LR, Han YM, Prather RS, Day BN: Morphologic evaluation and actin filament distribution in porcine embryos produced in vitro and in vivo. Biol Reprod 1999, 60:1020–1028
28. Ju JC, Tseng JK: Nuclear and cytoskeletal alterations of in vitro matured porcine oocytes under hyperthermia. Mol Reprod Dev 2004, 68:125–133
29. Ishibashi S, Sakaguchi M, Kuroiwa T, Yamasaki M, Kanemura Y, Shizuko I, Shimazaki T, Onodera M, Okano H, Mizusawa H: Human neural stem/progenitor cells, expanded in long-term neurosphere culture, promote functional recovery after focal ischemia in Mongolian gerbils. J Neurosci Res 2004, 78:215–223
30. Sun QY: Cellular and molecular mechanisms leading to cortical reaction and polyspermy block in mammalian eggs. Microsc Res Tech 2003, 61:342–348
31. Xia P, Wang Z, Yang Z, Tan J, Qin P: Ultrastructural study of polyspermy during early embryo development in pigs, observed by scanning electron microscope and transmission electron microscope. Cell Tissue Res 2001, 303:271–275
32. Sherrer ES, Rathbun TJ, Davis DL: Fertilization and blastocyst development in oocytes obtained from prepubertal and adult pigs. J Anim Sci 2004, 82:102–108
33. Lambert C, Goudeau H, Franchet C, Lambert G, Goudeau M: Ascidian eggs block polyspermy by two independent mechanisms: one at the egg plasma membrane, the other involving the follicle cells. Mol Reprod Dev 1997, 48:137–143
34. Wang WH, Abeydeera LR, Prather RS, Day BN: Morphologic comparison of ovulated and in vitro-matured porcine oocytes, with particular reference to polyspermy after in vitro fertilization. Mol Reprod Dev 1998, 49:308–316
35. Hatanaka Y, Nagai T, Tobita T, Nakano M: Changes in the properties and composition of zona pellucida of pigs during fertilization in vitro. J Reprod Fertil 1992, 95:431–440
36. Sengoku K, Tamate K, Horikawa M, Takaoka Y, Ishikawa M, Dukelow WR: Plasma membrane block to polyspermy in human oocytes and preimplantation embryos. J Reprod Fertil 1995, 105:85–90
37. Horvath PM, Kellom T, Caulfield J, Boldt J: Mechanistic studies of the plasma membrane block to polyspermy in mouse eggs. Mol Reprod Dev 1993, 34:65–72
38. Ducibella T: The cortical reaction and development of activation competence in mammalian oocytes. Hum Reprod Update 1996, 2:29–42
39. Miyado K, Yamada G, Yamada S, Hasuwa H, Nakamura Y, Ryu F, Suzuki K, Kosai K, Inoue K, Ogura A, Okabe M, Mekada E: Requirement of CD9 on the egg plasma membrane for fertilization. Science 2000, 287:321–324
40. Chen MS, Tung KS, Coonrod SA, Takahashi Y, Bigler D, Chang A, Yamashita Y, Kincade PW, Herr JC, White JM: Role of the integrin-associated protein CD9 in binding between sperm ADAM 2 and the egg integrin alpha6beta1: implications for murine fertilization. Proc Natl Acad Sci USA 1999, 96:11830–11835
41. Li YH, Hou Y, Ma W, Yuan JX, Zhang D, Sun QY, Wang WH: Localization of CD9 in pig oocytes and its effects on sperm-egg interaction. Reproduction 2004, 127:151–157
42. Hicke L, Dunn R: Regulation of membrane protein transport by ubiquitin and ubiquitin-binding proteins. Annu Rev Cell Dev Biol 2003, 19:141–172
43. Gava N, Clarke CL, Byth K, Arnett-Mansfield RL, deFazio A: Expression of progesterone receptors A and B in the mouse ovary during the estrous cycle. Endocrinology 2004, 145:3487–3494
44. Grasso P, Reichert Jr LE: In vivo effects of follicle-stimulating hormone-related synthetic peptides on the mouse estrous cycle. Endocrinology 1996, 137:5370–5375
45. Robertson SA, Mayrhofer G, Seamark RF: Ovarian steroid hormones regulate granulocyte-macrophage colony-stimulating factor synthesis by uterine epithelial cells in the mouse. Biol Reprod 1996, 54:183–196
46. Dean J, Cohen G, Kemp J, Robson L, Tembe V, Hasselaar J, Webster B, Lammi A, Smith A: Karyotype 69, XXX/47,XX,+15 in a 2 1/2 year old child. J Med Genet 1997, 34:246–249
47. Roberts HE, Saxe DF, Muralidharan K, Coleman KB, Zacharias JF, Fernhoff PM: Unique mosaicism of tetraploidy and trisomy 8: clinical, cytogenetic, and molecular findings in a live-born infant. Am J Med Genet 1996, 62:243–246
48. Isaksson R, Tiitinen A: Present concept of unexplained infertility. Gynecol Endocrinol 2004, 18:278–290

Available online at www.sciencedirect.com
ScienceDirect
Neurochemistry International 50 (2007) 119–129
NEUROCHEMISTRY International
www.elsevier.com/locate/neuint

Dopaminergic neuronal loss in transgenic mice expressing the Parkinson's disease-associated UCH-L1 I93M mutant

Rieko Setsuie [a,b,1], Yu-Lai Wang [a,1], Hideki Mochizuki [c,d], Hitoshi Osaka [a,e], Hideki Hayakawa [c], Nobutsune Ichihara [f], Hang Li [a], Akiko Furuta [a], Yae Sano [a,b], Ying-Jie Sun [a], Jungkee Kwon [a,g], Tomohiro Kabuta [a], Kenji Yoshimi [d], Shunsuke Aoki [a], Yoshikuni Mizuno [c,d], Mami Noda [b], Keiji Wada [a,*]

[a] *Department of Degenerative Neurological Diseases, National Institute of Neuroscience, National Center of Neurology and Psychiatory, Kodaira, Tokyo 187-8502, Japan*
[b] *Laboratory of Pathophysiology, Graduate School of Pharmaceutical Sciences, Kyushu University, Higashi-ku, Fukuoka 812-8582, Japan*
[c] *Department of Neurology, Juntendo University School of Medicine, Bunkyo-ku, Tokyo 113-8421, Japan*
[d] *Research Institute for Diseases of Old Age, Juntendo University School of Medicine, Bunkyo-ku, Tokyo 113-8421, Japan*
[e] *Division of Neurology, Clinical Research Institute, Kanagawa Children's Medical Center, Yokohama 232-8555, Japan*
[f] *Department of Anatomy, School of Veterinary Medicine, Azabu University, Sagamihara 229-8501, Japan*
[g] *College of Veterinary Medicine, Chonbuk National University, 644-14 Duckjin-Ku, Jeonju 561-756, Republic of Korea*

Received 14 March 2006; received in revised form 19 June 2006; accepted 11 July 2006
Available online 11 September 2006

Abstract

The I93M mutation in ubiquitin carboxyl-terminal hydrolase L1 (UCH-L1) was reported in one German family with autosomal dominant Parkinson's disease (PD). The causative role of the mutation has, however, been questioned. We generated transgenic (Tg) mice carrying human *UCHL1* under control of the *PDGF-B* promoter; two independent lines were generated with the I93M mutation (a high- and low-expressing line) and one line with wild-type human UCH-L1. We found a significant reduction in the dopaminergic neurons in the substantia nigra and the dopamine content in the striatum in the high-expressing I93M Tg mice as compared with non-Tg mice at 20 weeks of age. Although these changes were absent in the low-expressing I93M Tg mice, 1-methyl-4-phenyl-1,2,3,6-tetrahydropyridine (MPTP) treatment profoundly reduced dopaminergic neurons in this line as compared with wild-type Tg or non-Tg mice. Abnormal neuropathologies were also observed, such as silver staining-positive argyrophilic grains in the perikarya of degenerating dopaminergic neurons, in I93M Tg mice. The midbrains of I93M Tg mice contained increased amounts of insoluble UCH-L1 as compared with those of non-Tg mice, perhaps resulting in a toxic gain of function. Collectively, our data represent *in vivo* evidence that expression of $UCHL1^{I93M}$ leads to the degeneration of dopaminergic neurons.

Keywords: Ubiquitin carboxy-terminal hydrolase L1; Animal model; Parkinson's disease; Dopaminergic neuron

1. Introduction

Parkinson's disease (PD) is the second most common human neurodegenerative disorder after Alzheimer's disease (AD) (Dauer and Przedborski, 2003; Vila and Przedborski, 2004). PD patients exhibit motor dysfunction, including slowed movement (bradykinesia), resting tremor, rigidity, and postural instability (Dauer and Przedborski, 2003). The pathological basis of PD is the progressive loss of dopaminergic neurons in the substantia nigra pars compacta, giving rise to a decrease in dopamine content in the striatum (Dauer and Przedborski, 2003). Although most cases of PD are sporadic, studies of familial PD have provided accumulating evidence for the molecular mechanisms of PD. Thus far, at least six proteins have been identified to cause familial PD: α-synuclein (Chartier-Harlin et al., 2004; Farrer et al., 2004; Ibanez et al., 2004; Kruger et al., 1998; Polymeropoulos et al., 1997; Singleton et al., 2003), UCH-L1 (Leroy et al., 1998), parkin (Kitada et al., 1998), DJ-1 (Bonifati et al., 2003), phosphatase

* Corresponding author. Tel.: +81 42 346 1715; fax: +81 42 346 1745.
E-mail address: wada@ncnp.go.jp (K. Wada).
[1] These authors contributed equally to this work.

0197-0186/$ – see front matter © 2006 Elsevier Ltd. All rights reserved.
doi:10.1016/j.neuint.2006.07.015

and tensin homolog induced kinase-1 (PINK1) (Valente et al., 2004), and leucine-rich repeat kinase-2 (LRRK2) (Paisan-Ruiz et al., 2004; Zimprich et al., 2004). α-Synuclein, UCH-L1 and LRRK2 are linked to the autosomal dominant form of PD, whereas parkin, DJ-1 and PINK1 are linked to the recessive form.

In 1998, UCH-L1 carrying an Ile to Met mutation at amino acid position 93 (I93M) was identified in one German family affected by autosomal dominant familial PD. UCH-L1, also known as PGP9.5, is an abundant protein in neuronal cells, comprising up to about 1–2% of total protein in the brain. Its function as de-ubiquitylating enzyme (Larsen et al., 1998; Wilkinson et al., 1989), ubiquitylating enzyme (Liu et al., 2002), de-neddylating enzyme (Hemelaar et al., 2004), and mono-ubiquitin stabilizer (Osaka et al., 2003) has been reported. *In vitro* analysis using recombinant human UCH-L1 indicated that I93M mutation results in the reduction of hydrolase activity of about 50% (Nishikawa et al., 2003). *Uchl1* gene deletion in mice, however, was reported to causes gracile axonal dystrophy (*gad*), a recessive neurodegenerative disease with distinct phenotype and pathological features from PD (Saigoh et al., 1999). Moreover, extensive analysis failed to find other PD patients with mutations in the *UCHL1* gene (Lincoln et al., 1999; Maraganore et al., 1999) and there was an incomplete penetrance in reported German family (Leroy et al., 1998). Thus, the correlation of I93M mutation and pathogenesis of PD was questioned.

To elucidate the pathological role of UCH-L1^{I93M} expression in the pathogenesis of PD, *in vivo*, we generated transgenic mice expressing human UCH-L1^{I93M}.

2. Experimental procedures

2.1. Generation of *hUCHL1*^{WT} and *hUCHL1*^{I93M} transgenic mice

We generated transgenes by cloning either the wild-type or I93M mutant human UCH-L1 cDNAs under the control of the human platelet-derived growth factor B chain (*PDGF-B*) promoter (Fig. 1A) (Sasahara et al., 1991). Sequences encoding *UCHL1* were amplified from a human brain cDNA library (Stratagene, La Jolla, CA) by PCR and subcloned into the *Xho*I and *Not*I sites of pCI-neo (Promega, Madison, WI). The I93M substitution was obtained using QuikChange (Stratagene). The 5′ flanking region of the human *PDGF-B* chain gene was isolated from the human genomic DNA and inserted into the *Bgl*II and *Xho*I site of pCI-neo which results in the replacement of promoter from CMV to *PDGF-B*. The plasmid was linearized by digestion with *Hin*dIII and *Aat*II. A 2 μg/ml solution of the linearized plasmid of each transgene was then microinjected into the pronuclei of newly fertilized C57BL/6J mouse eggs. Offspring were screened for the presence of the transgene by PCR of tail DNA using specific primers (forward: PD-UCH-2, 5′-GCACTCTCCCTTCTCCTTTATA-3′; reverse: PD-UCH-5, 5′-CCTGTATGGCCTCATTCTTTTC-3′). Expression of hUCH-L1^{I93M} in a low-expressing mouse line only occurred in male mice. Thus, all experiments were done using male heterozygous transgenic mice. Animal care and handling were in accordance with institutional regulations for animal care and were approved by the Animal Investigation Committee of the National Institute of Neuroscience, National Center of Neurology and Psychiatry, Tokyo, Japan which conforms the National Institute of Health guide for the care and use of Laboratory animals.

2.2. Quantitative RT-PCR analysis

Primers specific for mouse *Uchl1* (forward: mL1-7, 5′-CCTTGGTTTGCAG-CTTTAGCA-3′; reverse: mL1-8, 5′-GGGCTGTAGAACGCAAGAAGA-3′) and human *UCHL1* (forward: L1Tg-F2, 5′-TGGCAACTTCTCCTCCTGCA-3′; reverse: L1Tg-R2, 5′-ACAGCACTTTGTTCAGCATC-3′) were designed, and SYBR Green-based real-time quantitative RT-PCR was performed using the ABI PRISM 7700 (Applied Biosystems, Foster City, CA) using total RNA from mouse brain ($n = 3$ for each line) (Aoki et al., 2002). GAPDH was used as an internal control.

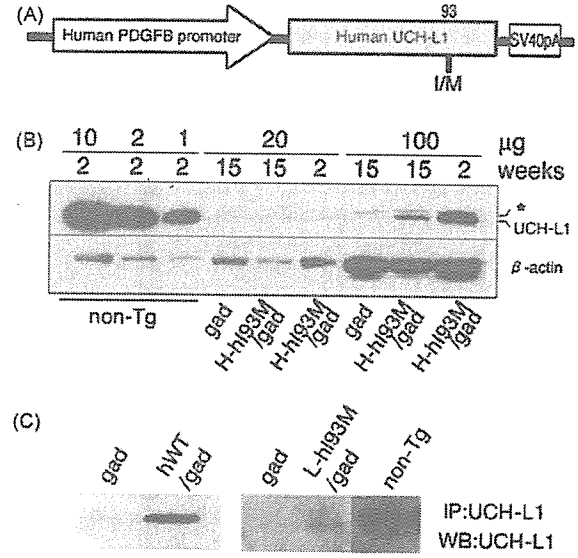

Fig. 1. Generation of transgenic mice expressing hUCH-L1^{WT}and hUCH-L1^{I93M}. (A) UCH-L1^{I93M} was constructed under control of the *PDGF-B* promoter, as depicted. (B) Immunoblotting analysis of endogenous mouse UCH-L1 and transgenic human UCH-L1 expression in mouse midbrain. To detect exogenous human UCH-L1 levels specifically, we generated transgenic mice in the *gad* background (H-hI93M/*gad*), which corresponds to the null mutant of *Uchl1*. Notice that the faint band corresponding to UCH-L1 is detected at 2 weeks of age when 20 μg protein/lane was loaded for the detergent-soluble fraction of midbrain origin in H-hI93M/*gad* mice. When the applied protein was increased to 100 μg/lane, UCH-L1 was easily detected at 2 weeks in H-hI93M/*gad* mice, and UCH-L1 levels markedly decreased by age 15 weeks. Faint bands indicated by the asterisk may correspond to UCH-L3, which cross-reacted with the UCH-L1 antibody when a large amount of protein was loaded per lane. (C) Immunoprecipitation analysis of exogenous human UCH-L1 in hWT/gad (left) and L-hI93M/gad (right) brains. Brain lysates from hWT/gad (left) or L-hI93M/gad (right) were both immunoprecipitated and detected using anti-UCH-L1 antibody. The band corresponding to the UCH-L1 can be found in both hWT/gad and L-hI93M/gad lysates but not in gad lysates indicating the exogenous human UCH-L1 expression.

2.3. Fractionation and immunoblotting and immunoprecipitation

For the immunoblotting of total UCH-L1, the soluble fraction in RIPA (20 mM Tris–HCl, pH 7.5; 0.1% SDS; 1.0% (w/v) Triton X-100; 1.0% sodium deoxycholate) with Complete EDTA-Free Protease Inhibitors (Roche, Basel, Switzerland) was extracted from H-hI93M/*gad* ([high-expressing] *UCH-L1*$^{I93M/-}$, *Uchl1*$^{gad/gad}$), *gad* and non-Tg mouse midbrains. The extracted samples were loaded as indicated in Fig. 1.

For subfractionation, the cortex and hippocampus were removed from the midbrains of a H-hI93M mouse or a non-Tg littermate and bottom half under the aqueduct were used as the substantia nigra fraction. The fractionation method was modified from that of Kahle et al. (2001). Each sample was homogenized with 9 volumes of 5% SDS/TBS lysis buffer (50 mM Tris–HCl (pH 7.5), 150 mM NaCl, 5% SDS) with Complete EDTA-Free Protease Inhibitors using a 23G syringe. After three times of 10 s sonication, samples were ultra-centrifuged in 130,000 × *g* for 1 h, and the supernatant were pooled as 5% SDS fraction. The pellets were washed with 5% SDS/TBS solution once and further homogenized in 8 M urea/5% SDS/TBS lysis buffer

(8 M urea, 5% SDS, 50 mM Tris–HCl (pH 7.5), 150 mM NaCl) with 23G syringe. The resulting supernatant was used as 8 M urea/5% SDS fraction. The protein concentration was assessed by a DC-protein assay kit (Bio-Rad). 1.25 μg of 5% SDS fraction and 0.5 μg of 8 M urea/5% SDS fraction were subjected to SDS-PAGE using 15% gels (Perfect NT Gel; DRC, Tokyo, Japan). Anti-UCH-L1 (1:5000, RA95101; Ultraclone, Isle of Wight, UK) and anti-β-actin (1:5000, clone AC15; Sigma, St. Louis, MO) were used to detect each protein. Signals were detected using a chemiluminescent SuperSignal West Dura Extended Duration Substrate kit or West Femto Maximum Sensitivity Substrate kit (Pierce, Rochford, IL) and analyzed with a ChemiImager (Alpha Innotech, San Leandro, CA). For the internal control of 8 M urea/5% SDS fraction, 1 μg protein were dot blotted to PVDF membrane and stained with Ponceau S staining (Rane et al., 2004). Statistical analyses were conducted using the two-tailed Student's *t*-test with total of four samples for each group.

For the immunoprecipitation, half of the brain (for hWT/gad) or midbrain region (for L-hI93M/gad) were homogenized in 2 ml ice-cold modified RIPA buffer (50 mM Tris–HCl, pH 7.4; 1% (w/v) Nonidet P40; 0.25% sodium deoxycholate; 150 mM NaCl; 1 mM EDTA) with Complete EDTA-Free Protease Inhibitors and centrifuged at 16,000 × *g* at 4 °C for 20 min. The protein concentration of the resulting supernatants was determined with the Protein Assay Kit (Bio-Rad, Hercules, CA). Immunoprecipitation was performed with a Seize X Mammalian Immunoprecipitation kit (Pierce, Rockford, IL) with some modifications. Briefly, 300 μg of protein was added to a 50 μl slurry of immobilized protein G cross-linked with rabbit polyclonal anti-human UCH-L1 (AB1716; Chemicon, Temecula, CA) or normal rabbit IgG and rotated at 4 °C overnight. The samples were then washed three times with 500 μl of 0.1B buffer (20 mM Tris–HCl, pH 8.0; 0.1 M KCl; 5 mM $MgCl_2$; 10% (w/v) glycerol; 0.1% (w/v) Tween 20; 10 mM β-mercaptoethanol). Elution of samples was performed by adding 20 μl of 5× SDS-PAGE sample buffer, and samples were boiled at 100 °C for 5 min.

2.4. Immunohistochemistry, immunofluorescence and electron microscopy

Brain and peripheral (sciatic) nerve sections from 2-, 7- and 20-week-old mice were analyzed ($n = 3$ for each line) by immunocytochemistry as previously described (Wang et al., 2004; Watanabe et al., 1977) using antibodies to UCH-L1 (1:4000; RA95101, Ultraclone), TH (1:1000; Chemicon) and ubiquitin (1:1000; Sigma–Aldrich, St. Louis, MO). Antibody binding was detected with 3,3′-diaminobenzidine tetrachloride (DAB) or 3-amino-9-ethylcarbazole (AEC) as a peroxidase substrate or Alexa-488- or Alexa-568-conjugated secondary antibodies (Invitrogen, Carlsbad, CA). Sections were then counterstained with hematoxylin. Ultrastructural electron microscopic studies of the substantia nigra were performed as described (Watanabe et al., 1977) using midbrain sections.

2.5. MPTP treatment

For MPTP treatment, the mice received four injections of 30 mg/kg MPTP–HCl intraperitoneally (Research Biochemicals, Natick, MA) in saline at 24-h intervals (Mochizuki et al., 2001).

2.6. Tyrosine hydroxylase-positive cell counting and biochemical analysis

Samples for both histochemistry and biochemical analysis were obtained from the same mouse. Each animal was deeply anesthetized with pentobarbital and perfused transcardially with 10 ml of ice-cold phosphate-buffered saline, and the brain was removed and divided into forebrain and midbrain–hindbrain regions.

For the tyrosine hydroxylase (TH)-positive cell counting, midbrain–hindbrain was fixed with chilled 4% formaldehyde solution (pH 7.4). The procedure of TH-positive cell counting was described previously (Furuya et al., 2004) with minor modifications. Briefly, the substantia nigra was cut into serial sections (30 μm), and every third section was subjected to immunostaining for TH using a polyclonal antibody to TH (a kind gift from I. Nagatsu, Fujita Health University, Aichi, Japan). The Vectorstain Elite ABC kit (Vector Labs, Burlingame, CA) was used for subsequent antibody detection with DAB as a peroxidase substrate. The number of viable TH-positive neurons was assessed by manual counting by a blind observer using coded slides (Furuya et al., 2004). The number of total neuronal cells outside the substantia nigra was counted after Bodian staining in the cerebral cortex (1 mm^2, seven regions per section), cerebellum (total of all lobules) and hippocampus (total number in CA1, CA2, CA3 and dentate gyrus). Statistical analysis were done by one-way ANOVA followed by post hoc test (Fisher's PLSD).

For the biochemical analysis, the striatum was quickly dissected from the forebrain, and the striatal tissue samples were weighed (~30 mg) and homogenized in 10 volumes (w/v) of ice-cold 0.05 M sodium acetate (pH 6.0). Homogenates were centrifuged (18,000 × *g*, 10 min at 4 °C), and the supernatant was frozen immediately on dry ice and stored frozen at −80 °C until use.

For the striatal dopamine measurement, supernatant (50 μl) from the striatal lysate was mixed with an equal volume of 0.2 M perchloric acid containing 0.2 mM EDTA and centrifuged (18,000 × *g*, 10 min at 4 °C), and the supernatant was applied to an HPLC system. Chromatographic separation was achieved using a C18 reversed-phase column (150 mm × 4.6 mm i.d., Model S-100; TOSOH, Tokyo, Japan). The mobile phase (50 mM citrate, 50 mM NaH_2PO_4, 0.1 mM EDTA, 4.36 mM 1-heptanesulfonate, 2.35% acetonitrile, 5.72% MeOH, pH 2.5) was pumped through the chromatographic system at a rate of 1.0 ml/min. A Coulochem electrode array system (ESA Inc., MA) with eight coulometric electrodes was used to quantify the eluted catecholamines and their metabolites. Statistical analysis was done by one-way ANOVA followed by post hoc test (Fisher's PLSD).

TH activity was assayed following the method of Hooper (1997) with minor modifications (Hooper et al., 1997; Naoi et al., 1988). The incubation mixture contained 50 μl of diluted sample and included the following components in a total volume of 200 μl: 0.2 M sodium acetate (pH 6.0), 0.2 M glycerol, 20,000 U/ml catalase, 1.0 mM 6-MPH4, 4.0 U/ml dihydropteridine reductase, 1 mM NADPH and 200 μM L-tyrosine. Incubations were carried out at 37 °C for 10 min in a shaking water bath. Reactions were terminated by adding 600 μl of ice-cold 0.33 M perchloric acid, 17 mM EDTA including 50 pmol of α-methyl DOPA as the internal standard. The L-DOPA produced was extracted onto alumina, and the catechols were eluted with 0.16 M acetic acid followed by 0.02 M phosphoric acid. A sample incubated on ice instead of 37 °C was used as a blank. The amount of L-DOPA was quantified with the HPLC system, as mentioned above. Statistical analysis was done by one-way ANOVA.

2.7. Silver staining

Sixty-micrometer brain sections from 12-week-old mice ($n = 3$ for each group) were stained using FD NeuroSilver kit (FD Neuro-Technologies, Catonsville, MD) according to the manufacturer's protocol to detect argyrophilic grain-positive degenerating neurons.

2.8. Behavioral tests

H-hI93M mice and non-Tg littermates were used for all behavioral analyses. For the accelerated rota-rod test, 20–25-week-old mice were placed on the rod (Ohara, Japan) at a speed of 5 rpm, and the speed was accelerated to 50 rpm in 5 min. The length of time that each mouse was able to remain on the rod before falling was recorded. For the locomotor activity test, 11–13-week-old or 20–23-week-old mice were placed separately in a home cage 4 days before the beginning of analysis for habituation. Two to four mice were monitored at once for locomotor activity on the home cage monitor (Ohara, Japan) for 63 h beginning from 5:30 p.m. All mice were housed with a 12 h light/dark cycle, with the light cycle beginning at 8 a.m. The last 12 h of active night were used for the analysis. Mice were weighed after the analysis; there were no differences between the weights H-hI93M and non-Tg mice (data not shown). Statistical analyses were conducted using the two-tailed Student's *t*-test.

3. Results

3.1. Generation of transgenic mice expressing human *UCHL1*^{I93M} in neurons of the substantia nigra

The human *PDGF-B* promoter was used to drive expression of the human *UCHL1* in Tg mice (Fig. 1A) (Sasahara et al., 1991). Germline transmission of *hUCHL1*^{I93M} was obtained in two independent Tg mouse lines (denoted L-hI93M and H-hI93M, where L and H denote low and high expression, respectively). Germline transmission of *hUCHL1*^{WT} was obtained in one Tg mouse line (denoted hWT). The levels of transgenic mRNA and endogenous *Uchl1* mRNA were assessed by quantitative RT-PCR using primers designed to amplify specifically the *UCHL1* transgene and mouse *Uchl1*, respectively. The estimated relative expression of *UCHL1* among the transgenic lines was H-hI93M > hWT > L-hI93M. The ratio of endogenous mouse *Uchl1* transcripts to transgenic human *UCHL1* transcripts was 111 in H-hI93M, 739 in hWT and 6015 in L-hI93M ($n = 3$ for each line).

At the amino acid level, human and mouse UCH-L1 differ at only 11 discrete positions, and endogenous UCH-L1 is one of the most abundant protein in the brain. Therefore, we were not able to make distinction between the exogenous human UCH-L1 and endogenous mouse UCH-L1 in the brains of Tg mice (data not shown) using immunoblotting analysis with several antibodies against human UCH-L1 from different companies (Chemicon; UltraClone; Medac; Biogenesis). To ascertain the expression of transgene product, we used *gad* mice, which lack endogenous UCH-L1 (Saigoh et al., 1999). We mated mice

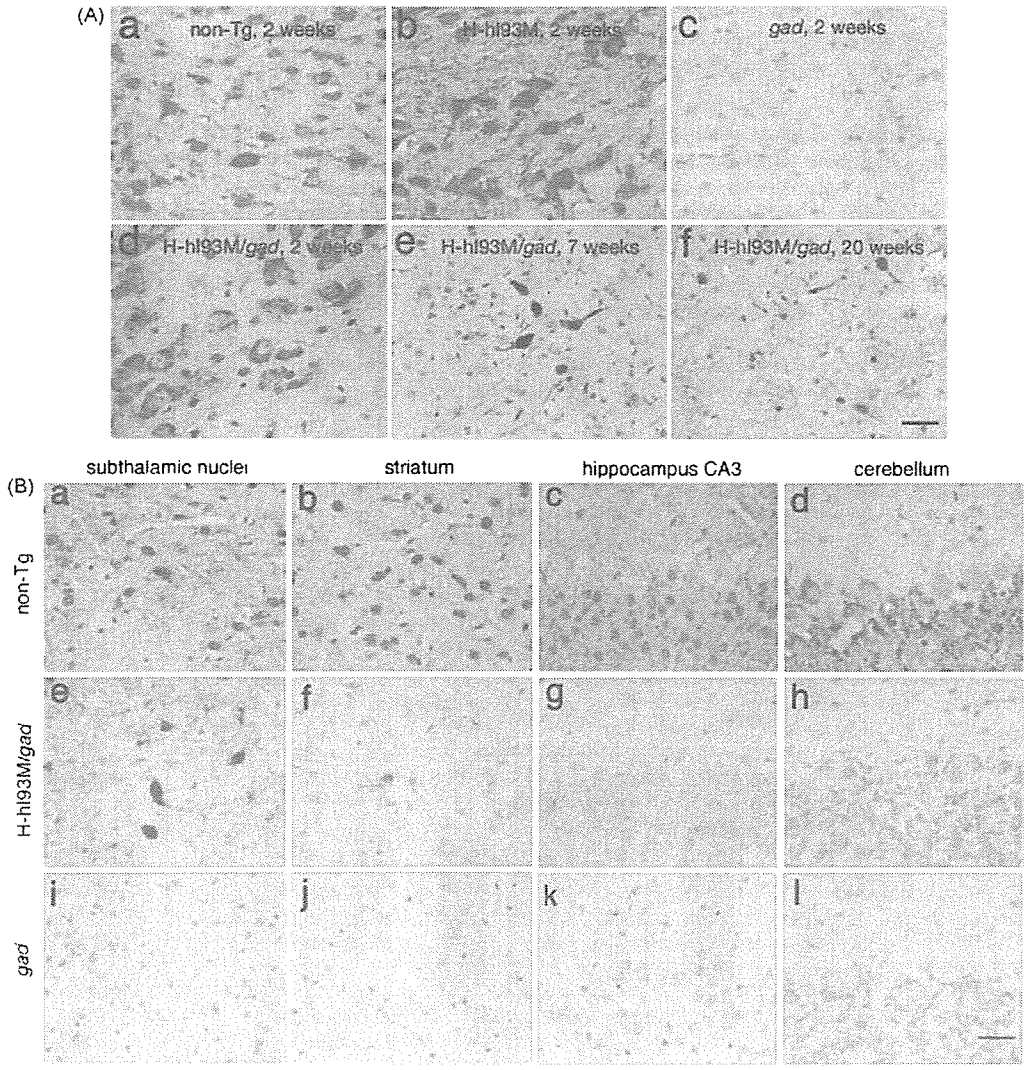

Fig. 2. Immunohistochemistry of UCH-L1 in coronal sections of the substantia nigra (A) and regions outside the substantia nigra (B) in H-hI93M, H-hI93M/*gad* and non-Tg mice. (A) Non-Tg mice (a), H-hI93M mice on a C57BL/6J background (b) and *gad* mice (c) at 2 weeks of age and H-hI93M/*gad* mice at 2 weeks (d), 7 weeks (e) and 20 weeks (f) of age. Neurons expressing UCH-L1 in the substantia nigra decreased in number and area, and densely stained neurons were observed in the aged substantia nigra. Scale bar: 30 μm. (B) UCH-L1 immunohistochemistry of coronal sections at the level of the subthalamic nuclei (a, e, i), striatum (b, f, j), hippocampus CA3 (c, g, k) and cerebellum (d, h, l). Upper row (a–d), non-Tg mice; middle row (e–h), H-hI93M/*gad* mice; lower row (i–l), *gad* mice. All mice were examined at 2 weeks of age. Scale bar: 30 μm.

from each transgenic line with mice homozygous for the *Uchl1*$^{gad/gad}$ allele (*gad* mice). Detergent-soluble (1% Triton X-100) fractions of mouse midbrain from H-hI93M/*gad* (*UCHL1*$^{I93M/-}$, *Uchl1*$^{gad/gad}$) at 2 and 15 weeks of age were subjected to SDS-PAGE and immunoblotted with anti-UCH-L1. We detected human UCH-L1 expression in H-hI93M/*gad* brains (Fig. 1B). Compared with endogenous mouse UCH-L1, which constitutes 1–2% of neuronal proteins, human UCH-L1 expression was substantially lower in H-hI93M/*gad* brains (~1% of endogenous UCH-L1 at 2 weeks of age; Fig. 1B). Interestingly, the level of transgenic human UCH-L1 was lower at 15 weeks than at 2 weeks of age (Fig. 1B). Although we could not detect human UCH-L1 in L-hI93M/*gad* and hWT/*gad* by standard immunoblotting methods, we were successful in detecting it by immunoprecipitation (Fig. 1C). These data suggest the expression of the human UCH-L1 in L-hI93M and hWT mice, which were much lower than in H-hI93M mice.

UCH-L1 is a cytosolic protein predominantly expressed in neuronal cells including dopaminergic neurons at substantia nigra with diffuse localization (data not shown). Thus, we next examined the immunohistochemical localization of the transgene products. In agreement with the data obtained by Western blotting analysis, UCH-L1-immunoreactive cells were not observed in any brain region, including the substantia nigra, of the L-hI93M/*gad* and hWT/*gad* mice (data not shown). In H-hI93M/*gad* mice, however, human UCH-L1^{I93M} was detected in the substantia nigra, the region that contains the central pathological lesions in PD, with relatively high intensities (Fig. 2A). Subthalamic nuclei, striatum, hippocampus CA3 and cerebellum also contained UCH-L1 immunoreactive cells in H-hI93M/*gad* mice (Fig. 2B). As with the previous report that CAT expression under control of the *PDGF-B* promoter in transgenic mice localizes to neuronal cell bodies (Sasahara et al., 1991), most UCH-L1-immunoreactive cells in H-hI93M/*gad* mice had a neuronal morphology (Fig. 2). Western blotting analysis of midbrain lysates showed a reduction of transgenic UCH-L1^{I93M} at 15 weeks of age as compared with that at 2 weeks in H-hI93M/*gad* mice (Fig. 1B). Thus, we also performed immunohistochemical analysis of UCH-L1 on substantia nigra from 2-, 7- and 20-week-old H-hI93M/*gad* mice. We found many UCH-L1-positive neurons at 2 weeks. The number of positive cells had decreased by 7 weeks, however, at which time small-sized and densely stained neurons were observed, and UCH-L1-positive cells were barely

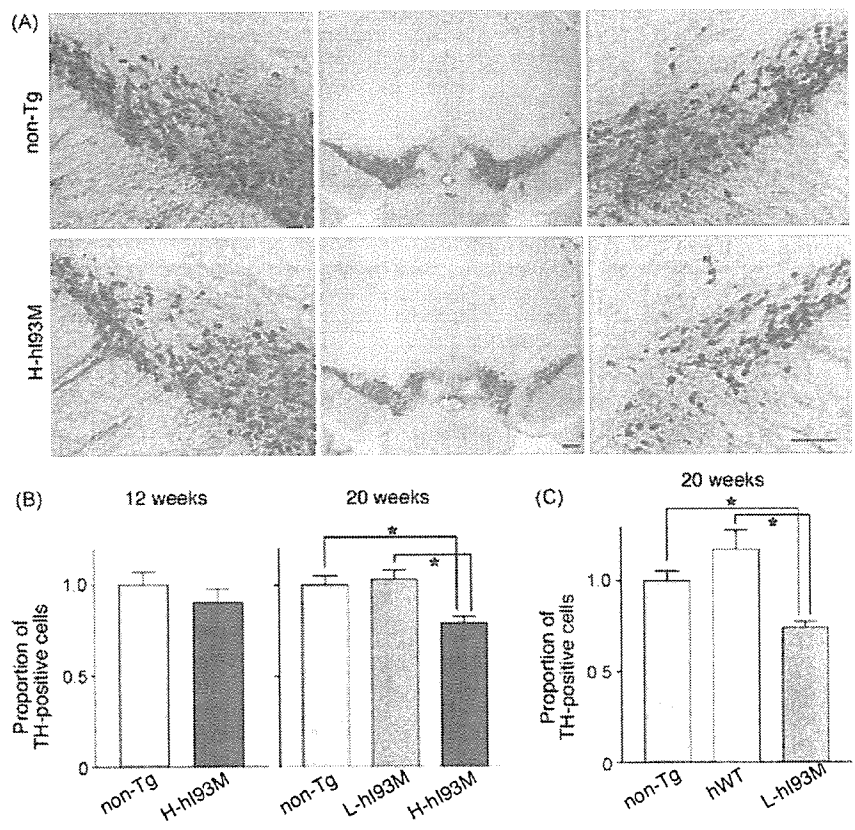

Fig. 3. TH-positive neurons of hI93M Tg mice were reduced as the animals aged. (A) Immunohistochemical staining of the substantia nigra with anti-TH in non-Tg (upper panels) and H-hI93M (lower panels) mice at 20 weeks of age. Scale bar: 1 mm. Left and right panels in the figure correspond to the left and right part of the middle panel, respectively. (B) Proportion of neurons stained with anti-TH in the substantia nigra from non-Tg and hI93M mice at 12 weeks (left panel) and 20 weeks (right panel) of age. Cell numbers were normalized to those for the non-Tg mice. Values are the mean ± S.E.M.; $n = 10$ Significance was examined by a one-way ANOVA. $^{*}p < 0.01$. (C) The number of TH-positive cells in the substantia nigra from 20-week-old non-Tg ($n = 5$), hWT ($n = 3$) and L-hI93M mice ($n = 5$) after treatment with MPTP. The cell numbers were normalized to those for non-Tg mice. Values are the mean ± S.E.M. Significance was examined by a one-way ANOVA. $^{*}p < 0.001$.

detectable at 20 weeks of age (Fig. 2A). Together, our results indicate that hUCH-L1^{I93M} is expressed in the neurons of the substantia nigra in H-hI93M mice, but the number of positive cells declines before 20 weeks of age. With the failure to detect hUCH-L1 protein in hWT/*gad* mice and L-hI93M/*gad* mice both in the Western blotting and the immunohistochemistry, we performed most of the analysis using H-hI93M mice with non-Tg mice as a control.

3.2. Loss of dopaminergic neurons in the substantia nigra of 20-week-old H-hI93M mice

We next determined whether the number of midbrain dopaminergic neurons was reduced in the substantia nigra of transgenic mice using TH immunohistochemistry. The number of TH-positive dopaminergic neurons in the substantia nigra at the same neuroanatomical level was compared and quantified for each transgenic mouse line. Surprisingly, we detected an ~30% reduction in TH-positive neurons in 20-week-old H-hI93M mice as compared with those in non-Tg control mice (Fig. 3A and B). This reduction was not seen in 12-week-old H-hI93M mice or 20-week-old L-hI93M mice. Together with the decrease in the level of UCH-L1^{I93M} (Fig. 1B) and the reduction in UCH-L1-positive neurons in the substantia nigra of H-hI93M/*gad* mice, our data indicate that UCH-L1^{I93M} expression in the dopaminergic neurons is sufficient to induce the degeneration of these neurons.

MPTP is a toxin used to induce an acute Parkinsonian syndrome that is indistinguishable from sporadic PD (Dauer and Przedborski, 2003). MPTP metabolite 1-methyl-4-pyridinium (MPP^+), an inhibitor of complex I of the mitochondrial respiration chain, is taken up by the terminals of dopaminergic neurons via the dopamine transporter (DAT), thereby causing the selective death of nigral neurons (Dauer and Przedborski, 2003). Although neuronal loss was not observed in L-hI93M mice at 20 weeks of age, we speculated that dopaminergic

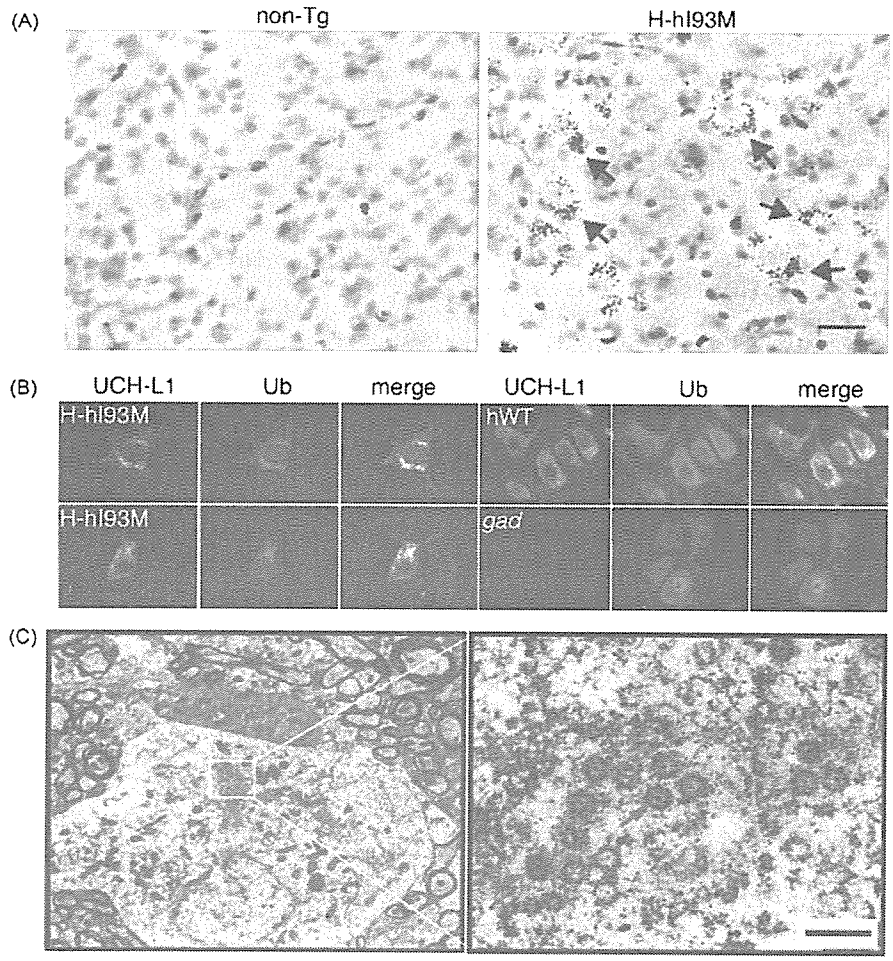

Fig. 4. Several neuropathological features reminiscent of PD are present in H-hI93M mice brains. (A) Silver staining of the substantia nigra at 12 weeks of age in non-Tg and H-hI93M mice. Note the presence of silver staining-positive argyrophilic grains in the cell bodies of some dopaminergic neurons in H-hI93M mice (arrows). This kind of abnormal structure was not seen in substantia nigra of non-Tg mice. Scale bar: 30 μm. (B) Confocal images of dopaminergic neurons from hWT, H-hI93M and *gad* mice. H-hI93M mice showed the formation of ubiquitin-positive cytoplasmic inclusions (red) co-localized with UCH-L1 staining (green) in the remaining nigral neurons at 20 weeks of age. Compared with the diffuse, reduced staining of ubiquitin in *gad* mice, nigral neurons from hWT mice also showed a diffuse pattern of staining but with fine small granular cytoplasmic staining (red) co-localized with UCH-L1 (green). (C) Electron micrographs of a nigral neuron from a 20-week-old H-hI93M mouse at the level of the cell body (left panel), and dense-core vesicles (red arrows) at higher magnification (right panel). Scale bar: 1 μm.

neurons of L-hI93M mice might be more susceptible to MPTP toxin compared to that of non-Tg mice or hWT mice. As expected, significantly fewer TH-positive neurons were observed in L-hI93M mice after MPTP treatment as compared with hWT or non-Tg control mice though hWT express higher *hUCHL1* compared to L-hI93M (Fig. 3C). The number of TH-positive neurons in MPTP-treated hWT mice was somewhat higher than that in non-Tg mice ($p < 0.001$). Taken together with the fact that expression of human UCH-L1 in L-hI93M is lower than that in hWT, these results suggest that the UCH-L1^{I93M} mutant, but not UCH-L1^{WT}, is specifically toxic to dopaminergic neurons.

3.3. Presence of neuropathology in dopaminergic neurons from H-hI93M mice

To evaluate the degenerative process of dopaminergic neurons, silver staining was used to indicate argyrophilic degenerating neurons (Lo Bianco et al., 2004). In non-Tg mice, no silver staining was observed, whereas scattered neurons containing grains that were silver staining positive were present in the substantia nigra of H-hI93M mice (Fig. 4A). The presence of intracellular inclusions called Lewy bodies and Lewy neurites are neuropathological characteristics of PD and are silver staining positive (Sandmann-Keil et al., 1999; Uchihara et al., 2005). It is also known that UCH-L1 and ubiquitin, as well as α-synuclein, are components of Lewy bodies (Lowe et al., 1990). Furthermore, UCH-L1 is tightly associated with mono-ubiquitin *in vivo* (Osaka et al., 2003). Thus, we expected that the silver staining-positive grains might have characteristic features of Lewy bodies. We therefore compared the immunohistochemical analysis of UCH-L1 and ubiquitin. Compared with reduced staining for ubiquitin in *gad* mice, strong and diffuse ubiquitin staining was observed in nigral neurons of hWT mice and non-Tg mice (data not shown), and this staining co-localized with UCH-L1, which is in agreement with our previous report (Osaka et al., 2003). In H-hI93M substantia nigra at 20 weeks of age, ubiquitin- and UCH-L1-positive cytoplasmic inclusions, a large aggregates with different morphology from small dots usually seen in hWT mice and non-Tg mice, were observed in a portion of the remaining nigral neurons (Fig. 4B). These inclusions were, however, α-synuclein or hematoxylin–eosin (HE) negative (data not shown). We could not observe UCH-L1- and ubiquitin-positive inclusions in L-hI93M mice (data not shown).

Another cellular characteristic of PD neuropathology is dense-core vesicles of about 80–200 nm in perikarya, which are frequently observed along with Lewy bodies in PD patients (Watanabe et al., 1977). We observed electron dense-core vesicles in the cytoplasm of ~30% of nigral neurons in H-hI93M mice using electron microscopy (Fig. 4C). In non-Tg mice, such vesicles with a similar shape were not detected in cell bodies but rather were seen in synaptic terminals. Taken together, our data indicate that degenerating dopaminergic neurons in the substantia nigra of H-hI93M mice are devoid of Lewy bodies but show some neuropathological features such as silver staining-positive argyrophilic grains, aggregates with UCH-L1 and ubiquitin, and dense-core vesicles in the perikarya.

3.4. Increased amount of SDS-insoluble but urea/SDS-soluble UCH-L1 in the midbrain of H-hI93M mice

UCH-L1^{I93M} has reduced α-helical content as compared with UCH-L1^{WT} (Nishikawa et al., 2003), and UCH-L1^{I93M} overexpression in COS7 cells results in more cells that contain cytoplasmic inclusions (Ardley et al., 2004). Thus, the presence of UCH-L1-positive inclusions in H-hI93M dopaminergic neurons led us to speculate whether UCH-L1^{I93M} would be less soluble than the wild-type protein *in vivo*. To biochemically characterize the changes in UCH-L1 deposited in the brains of H-hI93M mice, we sequentially extracted frozen midbrain tissues with 5% SDS (soluble fraction) and 8 M urea/5% SDS (insoluble fraction) and analyzed each fraction by immunoblotting with anti-UCH-L1. As expected, immunoblots of insoluble fractions showed a modest but statistically significant increase in UCH-L1 in the midbrains of H-hI93M mice as compared with those from a non-Tg mouse (Fig. 5A and B), indicating increased insolubility of UCH-L1^{I93M} *in vivo*, which might have resulted in dopaminergic neurotoxicity.

3.5. Decreased dopamine content in the striata of H-hI93M mice

Because the nigro-striatal pathway is severely affected in PD patients, and because our mice showed the degeneration of dopaminergic neurons in the substantia nigra, we evaluated the nerve terminals in the striatal pathway using

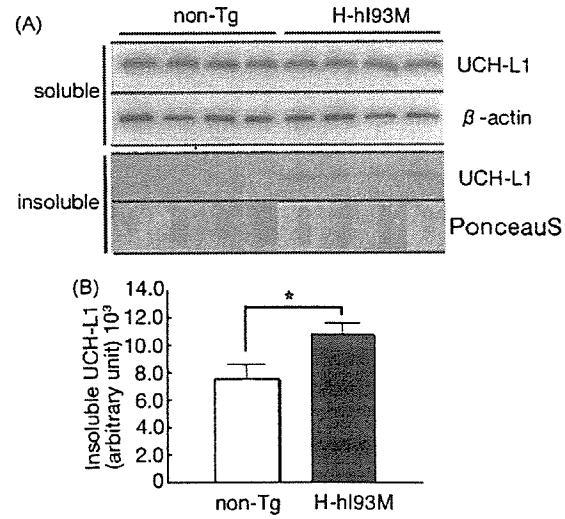

Fig. 5. Protein insolubility of UCH-L1 in H-hI93M Tg mice. (A) Immunoblotting analysis of UCH-L1 in soluble (5% SDS soluble) and insoluble (5% SDS insoluble and 8 M urea/5% SDS soluble) fractions from tissue containing the substantia nigra (11–13 weeks). Soluble fraction (5 μg for each) was probed with anti-UCH-L1 or anti-β-actin. Insoluble fraction (0.5 μg for each) was probed with anti-UCH-L1. One microgram of each insoluble fraction was applied to dot blotting and stained by Ponceau S to show that each fraction contained the same amount of total protein. A slight increase in the insolubility of UCH-L1 in the substantia nigra fraction from H-hI93M mice is seen as compared with that from non-Tg mice. (B) The experiment was done with H-hI93M mice and non-Tg littermates from five different litters, and the results of quantitative analyses in insoluble fraction is shown ($n = 5$ mice for each group).

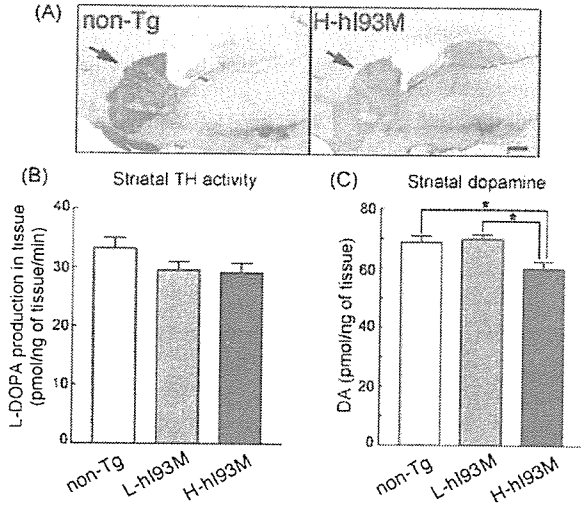

Fig. 6. H-hI93M mice show pathology in the striatum. Dopamine content and TH activity were lower in H-hI93M mice. (A) Sagittal sections from non-Tg and H-hI93M mice at 20 weeks of age were immunostained with the dopaminergic marker anti-TH. TH immunoreactivity is decreased in the nigro-striatal axons (arrows) of H-hI93M brains. Scale bar: 100 μm. (B) TH activity and (C) dopamine content were measured following extraction and homogenization of the mouse striatum of non-Tg, L-hI93M and H-hI93M mice at 20 weeks of age ($n = 4$; mean ± S.E). Significance was examined by a one-way ANOVA. $^{*}p < 0.05$.

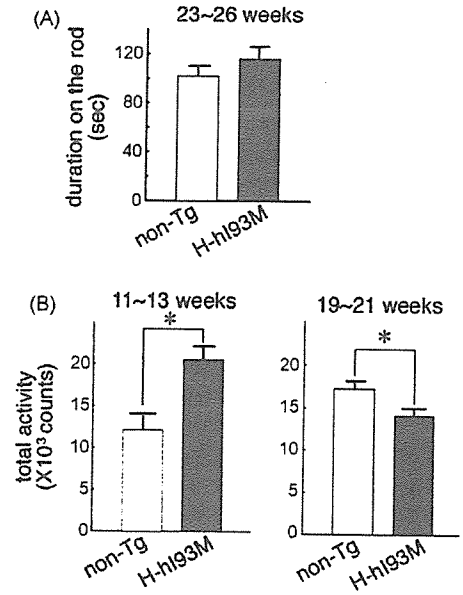

Fig. 7. H-hI93M transgenic mice show locomotor deficits. (A) Accelerated rota-rod analysis of H-hI93M and non-Tg mice ($n = 6$ for non-Tg and $n = 7$ for H-hI93M) at 23–26 weeks of age. Mice were placed on a rod, and their duration on the rod before falling off (mean value of three trials for each animal) was recorded. (B) Home cage monitor analysis of H-hI93M and non-Tg mice at 11–13 weeks of age (left; $n = 4$ for each line) and at 19–21 weeks of age (right; $n = 8$ for non-Tg and $n = 10$ for H-hI93M). Note the significant hypolocomotion of H-hI93M mice as compared with non-Tg mice at 19–21 weeks of age. Values are the mean ± S.E.M. Significance was examined using the unpaired Student's t-test. $^{*}p < 0.05$.

immunohistochemical and biochemical analyses. In agreement with the reduction of TH-positive dopaminergic neurons in the substantia nigra, nigro-striatal fibers in H-hI93M mice showed decreased immunoreactivity for TH as compared with that of non-Tg mice (Fig. 6A). TH activity, analyzed by determining L-DOPA production in the striatal tissues, also showed a tendency to decline in H-hI93M mice, although it was not significantly different (Fig. 6B). Loss of dopaminergic neurons in the substantia nigra and decreased TH activity in the striatum of H-hI93M mice prompted us to examine the concentration of striatal dopamine. Compared with non-Tg mice, H-hI93M mice showed a significant reduction of dopamine content in the striatum (Fig. 6C).

3.6. Decreased spontaneous, voluntary movements of H-hI93M mice

Given the prominent loss of dopaminergic neurons in the substantia nigra and the reduction in dopamine content in the striatum of H-hI93M mice, we next assessed the locomotor abilities of H-hI93M mice using a battery of well-established behavioral tests. Involuntary movement was analyzed by the rota-rod test (Goldberg et al., 2005) on 23–26-week-old mice. H-hI93M mice and non-Tg mice were similarly able to maintain their balance on the rotating rod during rod acceleration before falling off (Fig. 7A). We next analyzed spontaneous, voluntary movements with a locomotor activity test (Goldberg et al., 2005). Unexpectedly, 11–13-week-old H-hI93M mice showed significant hyperlocomotion during active periods (i.e., at night) as compared with non-Tg mice during home cage monitoring (Fig. 7B). However, 19–21-week-old H-hI93M mice showed a modest but significant reduction in locomotor activity during active periods as compared with non-Tg mice (Fig. 7B). These results indicate that, in addition to the neuropathological changes, H-hI93M mice exhibit mild behavioral deficits related to PD.

4. Discussion

In this study, we characterized transgenic mice expressing hUCH-L1^{I93M}, a mutation with presumptive association with familial PD, in the brain. Our previous attempt of making mouse UCH-L1^{WT} Tg mice under various higher expressing promoters, such as EF1α, resulted in an infertility of mice, thus it was impossible to maintain the lines. This failure resulted from the effect of overexpressing UCH-L1 in the testis/ovary leading to an increased apoptosis in these reproductive organs, although we did not find obvious morphological differences in the brain (Wang et al., 2006). Thus, we used *PDGF-B* promoter in this study to avoid massive expression of the transgene.

Two lines of hUCH-L1^{I93M} Tg mice and one line of hUCH-L1^{WT} Tg mice were viable and fertile without any predictable abnormalities. All of the three Tg lines expressed very limited levels of the human *UCHL1* gene with a maximum transcript ratio of about 1/100 as compared with the endogenous mouse *Uchl1*. However, immunohistological analysis indicated that higher level of hUCH-L1^{I93M} expression could be detected in the large number of neurons in the substantia nigra of

H-hI93M/gad mice at 2 weeks of age. In addition, there is a difference in the morphology of hUCH-L1^{I93M} expressing neurons, reminiscent of dying neurons, in the substantia nigra of H-hI93M/gad mice among 7 and 20 weeks of age. We also observed an eventual decline in the number of UCH-L1-positive neurons in H-hI93M/gad mice, as they age. Furthermore, the dopaminergic neurons in the substantia nigra of H-hI93M mice at 12 weeks of age showed silver staining-positive argylophilic grains, which represent neurons undergoing degeneration (Lo Bianco et al., 2004). Since we observed a loss of dopaminergic neurons in the substantia nigra and reduced dopamine content in the striatum of H-hI93M mice at 20 weeks of age, our results indicate the possibility that hUCH-L1^{I93M} expressing dopaminergic neurons degenerate with age.

In addition to cell loss, several neuropathological features were observed in the substantia nigra of H-hI93M mice. Dopaminergic neurons had (1) electron dense-core vesicles in the perikarya, and (2) cytoplasmic inclusions that were positive for both UCH-L1 and ubiquitin. Despite these features, we did not observe eosinophilic or α-synuclein-positive Lewy bodies at the substantia nigra in our morphological analyses. Thus, the mouse dopaminergic neurons expressing UCH-L1^{I93M} may die prior to the formation of Lewy bodies, or those mice might form these structures at stages beyond the period of our study.

The mechanisms responsible for dopaminergic cell loss in the substantia nigra of H-hI93M mice remain elusive. The I93M mutation in UCH-L1 reduces its hydrolase activity by about 50%, which has been suggested as a cause for the pathogenesis of PD (Nishikawa et al., 2003). However, we have not found clear evidence for nigro-striatal dopaminergic pathology in *gad* mice (data not shown). Since expression of UCH-L1 is not detected in gad mice, the reduction of hydrolase activity alone would not be the cause of PD. In light of our finding here that transgenic expression of UCH-L1^{I93M} results in dopaminergic pathology in mice, it would seem that this mutation elicits a gain of toxic function leading to the neuronal toxicity in the substantia nigra.

Our previous work using circular dichroism suggests that the I93M mutation reduces the α-helical content of UCH-L1 (Nishikawa et al., 2003). Recently, we had also showed, using small-angle neutron scattering, that wild-type or I93M mutant UCH-L1 exists as a dimmer in an aqueous solution. Moreover, their configuration differed; wild-type UCH-L1 has ellipsoidal shape where as I93M mutant has more globular shape (Naito et al., 2006). Cells expressing UCH-L1^{I93M} are more prone to form inclusions (Ardley et al., 2004). Proteomic analysis of autopsied brains from PD patients and AD patients shows that UCH-L1 is extensively modified by carbonyl formation, methionine oxidation and cysteine oxidation in the diseased brains (Choi et al., 2004). These modifications are shown to result from oxidative stress (Choi et al., 2004). We show here that I93M mutation in UCH-L1 increases its insolubility *in vivo*. From the very limited expression of human UCH-L1 I93M, it is possible to speculate that endogenous mouse UCH-L1 might become insoluble in the presence of I93M UCH-L1. In addition, L-hI93M neurons were more susceptible than hWT or non-Tg neurons to MPTP, an inhibitor of complex I. This observation suggests that UCH-L1^{I93M} easily gains toxicity under oxidative stress. The conformational change and/or the additional methionine oxidation in UCH-L1 caused by I93M mutation may cause increased insolubility and lead to the gain of a toxic function.

In addition, our behavioral analysis revealed that H-hI93M mice exhibit very slight defects in spontaneous, voluntary movement, as shown by their hyperlocomotion at 11–13 weeks of age and by their hypolocomotion at 19–21 weeks of age in the home cage monitor test. Patients with PD exhibit no clinical symptoms until 70–80% of dopaminergic neurons are lost (Dauer and Przedborski, 2003). Thus, the level of dopaminergic neuronal loss seen in H-hI93M mice might not be sufficient to produce severe clinical phenotypes. It is difficult to explain the hyperlocomotion detected at 11–13 weeks of age, by simple changes in the nigro-striatal pathway. Other brain areas might be related to the locomotor changes seen in H-hI93M mice. We will need further analysis to connect the dopaminergic cell loss and defects in spontaneous, voluntary movement in H-hI93M mice.

In attempts to replicate neuropathological aspects of PD, several of the familial PD genes have been altered in mice. Up to date, α-synuclein Tg mice with or without mutation (Fernagut and Chesselet, 2004), parkin knockout mice (Goldberg et al., 2003; Itier et al., 2003; Palacino et al., 2004; Perez and Palmiter, 2005; Von Coelln et al., 2004), and DJ-1 knockout mice (Chen et al., 2005; Goldberg et al., 2005; Kim et al., 2005) have been reported. Although these mice show some alterations in the function of dopaminergic neurons, none has dopaminergic neuron loss in the substantia nigra. Thus, we have developed the first mouse model with an alteration in a familial PD gene that leads to dopaminergic cell loss. Further analysis of these mice will help establish the role of UCH-L1 in PD, which may elucidate a common pathway for both familial and sporadic PD.

Acknowledgements

This work was supported by the Program for Promotion of Fundamental Studies in Health Sciences of the National Institute of Biomedical Innovation of Japan (KW); Grants-in-Aid for Scientific Research from the Ministry of Health, Labour and Welfare of Japan (KW); Grants-in-Aid for Scientific Research from the Ministry of Education, Culture, Sports, Science and Technology of Japan (KW); a grant from Japan Science and Technology Cooperation and a High Technology Research Center Grant (YM). We thank M. Shikama for the care and breeding of animals, H. Fujita for genotyping of animals, H. Kikuchi for technical assistance with tissue sections and N. Takagaki for the support in English. We also thank Dr. H. Hohjo for letting us use the home cage monitor.

References

Aoki, S., Su, Q., Li, H., Nishikawa, K., Ayukawa, K., Hara, Y., Namikawa, K., Kiryu-Seo, S., Kiyama, H., Wada, K., 2002. Identification of an axotomy-induced glycosylated protein, AIGP1, possibly involved in cell death triggered by endoplasmic reticulum-Golgi stress. J. Neurosci. 22, 10751–10760.

Ardley, H.C., Scott, G.B., Rose, S.A., Tan, N.G., Robinson, P.A., 2004. UCH-L1 aggresome formation in response to proteasome impairment indicates a role in inclusion formation in Parkinson's disease. J. Neurochem. 90, 379–391.

Bonifati, V., Rizzu, P., van Baren, M.J., Schaap, O., Breedveld, G.J., Krieger, E., Dekker, M.C., Squitieri, F., Ibanez, P., Joosse, M., van Dongen, J.W., Vanacore, N., van Swieten, J.C., Brice, A., Meco, G., van Duijn, C.M., Oostra, B.A., Heutink, P., 2003. Mutations in the DJ-1 gene associated with autosomal recessive early-onset parkinsonism. Science 299, 256–259.

Chartier-Harlin, M.C., Kachergus, J., Roumier, C., Mouroux, V., Douay, X., Lincoln, S., Levecque, C., Larvor, L., Andrieux, J., Hulihan, M., Waucquier, N., Defebvre, L., Amouyel, P., Farrer, M., Destee, A., 2004. Alpha-synuclein locus duplication as a cause of familial Parkinson's disease. Lancet 364, 1167–1169.

Chen, L., Cagniard, B., Mathews, T., Jones, S., Koh, H.C., Ding, Y., Carvey, P.M., Ling, Z., Kang, U.J., Zhuang, X., 2005. Age-dependent motor deficits and dopaminergic dysfunction in DJ-1 null mice. J. Biol. Chem. 280, 21418–21426.

Choi, J., Levey, A.I., Weintraub, S.T., Rees, H.D., Gearing, M., Chin, L.S., Li, L., 2004. Oxidative modifications and down-regulation of ubiquitin carboxyl-terminal hydrolase L1 associated with idiopathic Parkinson's and Alzheimer's diseases. J. Biol. Chem. 279, 13256–13264.

Dauer, W., Przedborski, S., 2003. Parkinson's disease: mechanisms and models. Neuron 39, 889–909.

Farrer, M., Kachergus, J., Forno, L., Lincoln, S., Wang, D.S., Hulihan, M., Maraganore, D., Gwinn-Hardy, K., Wszolek, Z., Dickson, D., Langston, J.W., 2004. Comparison of kindreds with parkinsonism and alpha-synuclein genomic multiplications. Ann. Neurol. 55, 174–179.

Fernagut, P.O., Chesselet, M.F., 2004. Alpha-synuclein and transgenic mouse models. Neurobiol. Dis. 17, 123–130.

Furuya, T., Hayakawa, H., Yamada, M., Yoshimi, K., Hisahara, S., Miura, M., Mizuno, Y., Mochizuki, H., 2004. Caspase-11 mediates inflammatory dopaminergic cell death in the 1-methyl-4-phenyl-1,2,3,6-tetrahydropyridine mouse model of Parkinson's disease. J. Neurosci. 24, 1865–1872.

Goldberg, M.S., Fleming, S.M., Palacino, J.J., Cepeda, C., Lam, H.A., Bhatnagar, A., Meloni, E.G., Wu, N., Ackerson, L.C., Klapstein, G.J., Gajendiran, M., Roth, B.L., Chesselet, M.F., Maidment, N.T., Levine, M.S., Shen, J., 2003. Parkin-deficient mice exhibit nigrostriatal deficits but not loss of dopaminergic neurons. J. Biol. Chem. 278, 43628–43635.

Goldberg, M.S., Pisani, A., Haburcak, M., Vortherms, T.A., Kitada, T., Costa, C., Tong, Y., Martella, G., Tscherter, A., Martins, A., Bernardi, G., Roth, B.L., Pothos, E.N., Calabresi, P., Shen, J., 2005. Nigrostriatal dopaminergic deficits and hypokinesia caused by inactivation of the familial Parkinsonism-linked gene DJ-1. Neuron 45, 489–496.

Hemelaar, J., Borodovsky, A., Kessler, B.M., Reverter, D., Cook, J., Kolli, N., Gan-Erdene, T., Wilkinson, K.D., Gill, G., Lima, C.D., Ploegh, H.L., Ovaa, H., 2004. Specific and covalent targeting of conjugating and deconjugating enzymes of ubiquitin-like proteins. Mol. Cell. Biol. 24, 84–95.

Hooper, D., Kawamura, M., Hoffman, B., Kopin, I.J., Hunyady, B., Mezey, E., Eisenhofer, G., 1997. Tyrosine hydroxylase assay for detection of low levels of enzyme activity in peripheral tissues. J. Chromatogr. B: Biomed. Sci. Appl. 694, 317–324.

Ibanez, P., Bonnet, A.M., Debarges, B., Lohmann, E., Tison, F., Pollak, P., Agid, Y., Durr, A., Brice, A., 2004. Causal relation between alpha-synuclein gene duplication and familial Parkinson's disease. Lancet 364, 1169–1171.

Itiėr, J.M., Ibanez, P., Mena, M.A., Abbas, N., Cohen-Salmon, C., Bohme, G.A., Laville, M., Pratt, J., Corti, O., Pradier, L., Ret, G., Joubert, C., Periquet, M., Araujo, F., Negroni, J., Casarejos, M.J., Canals, S., Solano, R., Serrano, A., Gallego, E., Sanchez, M., Denefle, P., Benavides, J., Tremp, G., Rooney, T.A., Brice, A., Garcia de Yebenes, J., 2003. Parkin gene inactivation alters behaviour and dopamine neurotransmission in the mouse. Hum. Mol. Genet. 12, 2277–2291.

Kahle, P.J., Neumann, M., Ozmen, L., Muller, V., Odoy, S., Okamoto, N., Jacobsen, H., Iwatsubo, T., Trojanowski, J.Q., Takahashi, H., Wakabayashi, K., Bogdanovic, N., Riederer, P., Kretzschmar, H.A., Haass, C., 2001. Selective insolubility of alpha-synuclein in human Lewy body diseases is recapitulated in a transgenic mouse model. Am. J. Pathol. 159, 2215–2225.

Kim, R.H., Smith, P.D., Aleyasin, H., Hayley, S., Mount, M.P., Pownall, S., Wakeham, A., You-Ten, A.J., Kalia, S.K., Horne, P., Westaway, D., Lozano, A.M., Anisman, H., Park, D.S., Mak, T.W., 2005. Hypersensitivity of DJ-1-deficient mice to 1-methyl-4-phenyl-1,2,3,6-tetrahydropyrindine (MPTP) and oxidative stress. Proc. Natl. Acad. Sci. U.S.A. 102, 5215–5220.

Kitada, T., Asakawa, S., Hattori, N., Matsumine, H., Yamamura, Y., Minoshima, S., Yokochi, M., Mizuno, Y., Shimizu, N., 1998. Mutations in the parkin gene cause autosomal recessive juvenile parkinsonism. Nature 392, 605–608.

Kruger, R., Kuhn, W., Muller, T., Woitalla, D., Graeber, M., Kosel, S., Przuntek, H., Epplen, J.T., Schols, L., Riess, O., 1998. Ala30Pro mutation in the gene encoding alpha-synuclein in Parkinson's disease. Nat. Genet. 18, 106–108.

Larsen, C.N., Krantz, B.A., Wilkinson, K.D., 1998. Substrate specificity of deubiquitinating enzymes: ubiquitin C-terminal hydrolases. Biochemistry 37, 3358–3368.

Leroy, E., Boyer, R., Auburger, G., Leube, B., Ulm, G., Mezey, E., Harta, G., Brownstein, M.J., Jonnalagada, S., Chernova, T., Dehejia, A., Lavedan, C., Gasser, T., Steinbach, P.J., Wilkinson, K.D., Polymeropoulos, M.H., 1998. The ubiquitin pathway in Parkinson's disease. Nature 395, 451–452.

Lincoln, S., Vaughan, J., Wood, N., Baker, M., Adamson, J., Gwinn-Hardy, K., Lynch, T., Hardy, J., Farrer, M., 1999. Low frequency of pathogenic mutations in the ubiquitin carboxy-terminal hydrolase gene in familial Parkinson's disease. Neuroreport 10, 427–429.

Liu, Y., Fallon, L., Lashuel, H.A., Liu, Z., Lansbury Jr., P.T., 2002. The UCH-L1 gene encodes two opposing enzymatic activities that affect alpha-synuclein degradation and Parkinson's disease susceptibility. Cell 111, 209–218.

Lo Bianco, C., Schneider, B.L., Bauer, M., Sajadi, A., Brice, A., Iwatsubo, T., Aebischer, P., 2004. Lentiviral vector delivery of parkin prevents dopaminergic degeneration in an alpha-synuclein rat model of Parkinson's disease. Proc. Natl. Acad. Sci. U.S.A. 101, 17510–17515.

Lowe, J., McDermott, H., Landon, M., Mayer, R.J., Wilkinson, K.D., 1990. Ubiquitin carboxyl-terminal hydrolase (PGP 9.5) is selectively present in ubiquitinated inclusion bodies characteristic of human neurodegenerative diseases. J. Pathol. 161, 153–160.

Maraganore, D.M., Farrer, M.J., Hardy, J.A., Lincoln, S.J., McDonnell, S.K., Rocca, W.A., 1999. Case-control study of the ubiquitin carboxy-terminal hydrolase L1 gene in Parkinson's disease. Neurology 53, 1858–1860.

Mochizuki, H., Hayakawa, H., Migita, M., Shibata, M., Tanaka, R., Suzuki, A., Shimo-Nakanishi, Y., Urabe, T., Yamada, M., Tamayose, K., Shimada, T., Miura, M., Mizuno, Y., 2001. An AAV-derived Apaf-1 dominant negative inhibitor prevents MPTP toxicity as antiapoptotic gene therapy for Parkinson's disease. Proc. Natl. Acad. Sci. U.S.A. 98, 10918–10923.

Naito, S., Mochizuki, H., Yasuda, T., Mizuno, Y., Furusaka, M., Ikeda, S., Adachi, T., Shimizu, H.M., Suzuki, J., Fujiwara, S., Okada, T., Nishikawa, K., Aoki, S., Wada, K., 2006. Characterization of multimetric variants of ubiquitin carboxyl-terminal hydrolase L1 in water by small-angle neutron scattering. Biochem. Biophys. Res. Commun. 339, 717–725.

Naoi, M., Takahashi, T., Nagatsu, T., 1988. Simple assay procedure for tyrosine hydroxylase activity by high-performance liquid chromatography employing coulometric detection with minimal sample preparation. J. Chromatogr. 427, 229–238.

Nishikawa, K., Li, H., Kawamura, R., Osaka, H., Wang, Y.L., Hara, Y., Hirokawa, T., Manago, Y., Amano, T., Noda, M., Aoki, S., Wada, K., 2003. Alterations of structure and hydrolase activity of parkinsonism-associated human ubiquitin carboxyl-terminal hydrolase L1 variants. Biochem. Biophys. Res. Commun. 304, 176–183.

Osaka, H., Wang, Y.L., Takada, K., Takizawa, S., Setsuie, R., Li, H., Sato, Y., Nishikawa, K., Sun, Y.J., Sakurai, M., Harada, T., Hara, Y., Kimura, I., Chiba, S., Namikawa, K., Kiyama, H., Noda, M., Aoki, S., Wada, K., 2003. Ubiquitin carboxy-terminal hydrolase L1 binds to and stabilizes monoubiquitin in neuron. Hum. Mol. Genet. 12, 1945–1958.

Paisan-Ruiz, C., Jain, S., Evans, E.W., Gilks, W.P., Simon, J., van der Brug, M., Lopez de Munain, A., Aparicio, S., Gil, A.M., Khan, N., Johnson, J., Martinez, J.R., Nicholl, D., Carrera, I.M., Pena, A.S., de Silva, R., Lees, A., Marti-Masso, J.F., Perez-Tur, J., Wood, N.W., Singleton, A.B., 2004. Cloning of the gene containing mutations that cause PARK8-linked Parkinson's disease. Neuron 44, 595–600.

Palacino, J.J., Sagi, D., Goldberg, M.S., Krauss, S., Motz, C., Wacker, M., Klose, J., Shen, J., 2004. Mitochondrial dysfunction and oxidative damage in parkin-deficient mice. J. Biol. Chem. 279, 18614–18622.

Perez, F.A., Palmiter, R.D., 2005. Parkin-deficient mice are not a robust model of parkinsonism. Proc. Natl. Acad. Sci. U.S.A. 102, 2174–2179.

Polymeropoulos, M.H., Lavedan, C., Leroy, E., Ide, S.E., Dehejia, A., Dutra, A., Pike, B., Root, H., Rubenstein, J., Boyer, R., Stenroos, E.S., Chandrasekharappa, S., Athanassiadou, A., Papapetropoulos, T., Johnson, W.G., Lazzarini, A.M., Duvoisin, R.C., Di Iorio, G., Golbe, L.I., Nussbaum, R.L., 1997. Mutation in the alpha-synuclein gene identified in families with Parkinson's disease. Science 276, 2045–2047.

Rane, N.S., Yonkovich, J.L., Hegde, R.S., 2004. Protection from cytosolic prion protein toxicity by modulation of protein translocation. EMBO J. 23, 4550–4559.

Saigoh, K., Wang, Y.L., Suh, J.G., Yamanishi, T., Sakai, Y., Kiyosawa, H., Harada, T., Ichihara, N., Wakana, S., Kikuchi, T., Wada, K., 1999. Intragenic deletion in the gene encoding ubiquitin carboxy-terminal hydrolase in gad mice. Nat. Genet. 23, 47–51.

Sandmann-Keil, D., Braak, H., Okochi, M., Haass, C., Braak, E., 1999. Alpha-synuclein immunoreactive Lewy bodies and Lewy neurites in Parkinson's disease are detectable by an advanced silver-staining technique. Acta Neuropathol. (Berl.) 98, 461–464.

Sasahara, M., Fries, J.W., Raines, E.W., Gown, A.M., Westrum, L.E., Frosch, M.P., Bonthron, D.T., Ross, R., Collins, T., 1991. PDGF B-chain in neurons of the central nervous system, posterior pituitary, and in a transgenic model. Cell 64, 217–227.

Singleton, A.B., Farrer, M., Johnson, J., Singleton, A., Hague, S., Kachergus, J., Hulihan, M., Peuralinna, T., Dutra, A., Nussbaum, R., Lincoln, S., Crawley, A., Hanson, M., Maraganore, D., Adler, C., Cookson, M.R., Muenter, M., Baptista, M., Miller, D., Blancato, J., Hardy, J., Gwinn-Hardy, K., 2003. Alpha-synuclein locus triplication causes Parkinson's disease. Science 302, 841.

Uchihara, T., Nakamura, A., Mochizuki, Y., Hayashi, M., Orimo, S., Isozaki, E., Mizutani, T., 2005. Silver stainings distinguish Lewy bodies and glial cytoplasmic inclusions: comparison between Gallyas-Braak and Campbell-Switzer methods. Acta Neuropathol. (Berl.) 110, 255–260.

Valente, E.M., Abou-Sleiman, P.M., Caputo, V., Muqit, M.M., Harvey, K., Gispert, S., Ali, Z., Del Turco, D., Bentivoglio, A.R., Healy, D.G., Albanese, A., Nussbaum, R., Gonzalez-Maldonado, R., Deller, T., Salvi, S., Cortelli, P., Gilks, W.P., Latchman, D.S., Harvey, R.J., Dallapiccola, B., Auburger, G., Wood, N.W., 2004. Hereditary early-onset Parkinson's disease caused by mutations in PINK1. Science 304, 1158–1160.

Vila, M., Przedborski, S., 2004. Genetic clues to the pathogenesis of Parkinson's disease. Nat. Med. 10 (Suppl.), S58–S62.

Von Coelln, R., Thomas, B., Savitt, J.M., Lim, K.L., Sasaki, M., Hess, E.J., Dawson, V.L., Dawson, T.M., 2004. Loss of locus coeruleus neurons and reduced startle in parkin null mice. Proc. Natl. Acad. Sci. U.S.A. 101, 10744–10749.

Wang, Y.L., Liu, W., Sun, Y.J., Kwon, J., Setsuie, R., Osaka, H., Noda, M., Aoki, S., Yoshikawa, Y., Wada, K., 2006. Overexpression of ubiquitin carboxyl-terminal hydrolase L1 arrests spermatogenesis in transgenic mice. Mol. Reprod. Develop. 73, 40–49.

Wang, Y.L., Takeda, A., Osaka, H., Hara, Y., Furuta, A., Setsuie, R., Sun, Y.J., Kwon, J., Sato, Y., Sakurai, M., Noda, M., Yoshikawa, Y., Wada, K., 2004. Accumulation of beta- and gamma-synucleins in the ubiquitin carboxyl-terminal hydrolase L1-deficient gad mouse. Brain Res. 1019, 1–9.

Watanabe, I., Vachal, E., Tomita, T., 1977. Dense core vesicles around the Lewy body in incidental Parkinson's disease: an electron microscopic study. Acta Neuropathol. (Berl.) 39, 173–175.

Wilkinson, K.D., Lee, K.M., Deshpande, S., Duerksen-Hughes, P., Boss, J.M., Pohl, J., 1989. The neuron-specific protein PGP 9.5 is a ubiquitin carboxyl-terminal hydrolase. Science 246, 670–673.

Zimprich, A., Biskup, S., Leitner, P., Lichtner, P., Farrer, M., Lincoln, S., Kachergus, J., Hulihan, M., Uitti, R.J., Calne, D.B., Stoessl, A.J., Pfeiffer, R.F., Patenge, N., Carbajal, I.C., Vieregge, P., Asmus, F., Muller-Minsk, B., Dickson, D.W., Meeting, T., Strom, T.M., Wszolek, Z.K., Gasser, T., 2004. Mutations in LRRK2 cause autosomal-dominant parkinsonism with allomorphic pathology. Neurone 44, 601–607.